Targeted deletion of GD3 synthase protects against MPTP-induced neurodegeneration

Yada Akkhawattanangkul[1], **Panchanan Maiti**[2], **Yi Xue**[2], **Dipendra Aryal**[4], **William C. Wetsel**[4], **David Hamilton**[1], **Stephen C. Fowler**[5], and **Michael P. McDonald**[2,3]

[1]Department of Comparative Medicine, University of Tennessee Health Science Center, Memphis, TN 38163

[2]Department of Neurology, University of Tennessee Health Science Center, Memphis, TN 38163

[3]Department of Anatomy & Neurobiology, University of Tennessee Health Science Center, Memphis, TN 38163

[4]Departments of Psychiatry & Behavioral Sciences, Cell Biology, and Neurobiology, Duke University Medical Center, Durham, NC 27710

[5]Department of Pharmacology & Toxicology, University of Kansas, Lawrence, KS 66045

Abstract

Parkinson's disease is a debilitating neurodegenerative condition for which there is no cure. Converging evidence implicates gangliosides in the pathogenesis of several neurodegenerative diseases, suggesting a potential new class of therapeutic targets. We have shown that interventions that simultaneously increase the neuroprotective GM1 ganglioside and decrease the pro-apoptotic GD3 ganglioside—such as inhibition of GD3 synthase (GD3S) or administration of sialidase—are neuroprotective *in vitro* and in a number of preclinical models. In the present study we investigated the effects of GD3S deletion on parkinsonism induced by 1-Methyl-4phenyl-1,2,3,6-tetrahydropyridine (MPTP). MPTP was administered to GD3S−/− mice or controls using a subchronic regimen consisting of three series of low-dose injections (11 mg/kg/day x 5 days each, 3 weeks apart), and motor function was assessed after each. The typical battery of tests used to assess parkinsonism failed to detect deficits in MPTP-treated mice. More sensitive measures— such as the force-plate actimeter and treadmill gait parameters—detected subtle effects of MPTP, some of which were absent in mice lacking GD3S. In wild-type mice MPTP destroyed 53% of the tyrosine-hydroxylase (TH)-positive neurons in the substantia nigra pars compacta (SNc) and reduced striatal dopamine 60.7%. In contrast, lesion size was only 22.5% in GD3S−/− mice and striatal dopamine was reduced by 37.2%. Stereological counts of Nissl-positive SNc neurons that did not express TH suggest that neuroprotection was complete but TH expression was suppressed in some cells. These results demonstrate that inhibition of GD3S has neuroprotective properties in the MPTP model may warrant further investigation as a therapeutic target.

Address correspondence to: Mike McDonald, PhD, UTHSC Department of Neurology, 855 Monroe Ave., 415 Link Bldg., Memphis, TN 38163, (901) 448-4648, mike@tennessee.edu.

Keywords

Parkinson's disease; gangliosides; MPTP; bradykinesia; motor function; neuroprotection; dopamine; substantia nigra

---

Introduction

Parkinson's disease is one of the most common neurodegenerative disorders of aging, characterized neuropathologically by progressive loss of dopaminergic neurons in substantia nigra pars compacta (SNc) and depletion of striatal dopamine (Anglade *et al.*, 1997; Bernheimer *et al.*, 1973; Forno *et al.*, 1986). Parkinsonian motor symptoms include akinesia, bradykinesia, rigidity, tremor, and gait impairment. Investigation into the pathogenesis of Parkinson's disease has intensified over the past few decades, but there is still no cure. Current therapies are only partially or transiently effective or are only effective in a minority of patients (Connolly & Lang, 2014; Lukins *et al.*, 2014; Poulopoulos *et al.*, 2012). None can stop the ongoing degenerative process.

The cause of dopaminergic cell death in Parkinson's disease is not known, although converging evidence implicates the ceramide/sphingomyelin-dependent apoptotic pathway (Abbott *et al.*, 2014; Anglade *et al.*, 1997; Ariga *et al.*, 1998; Brugg *et al.*, 1996; Mochizuki *et al.*, 1996). A number of papers have shown that *de novo* synthesis of GD3 ganglioside is required for Fas- and ceramide-mediated apoptosis (De Maria *et al.*, 1997; De Maria *et al.*, 1998; Melchiorri *et al.*, 2002; Morales *et al.*, 2004). We have shown that deleting *St8sia1*, the gene that codes for GD3 synthase (GD3S), protects against apoptosis induced by the 42-amino-acid amyloid-β sequence (Aβ42) or folate deficiency in primary neurons (Bernardo *et al.*, 2009). We have also shown that intraventricular infusion of sialidase from *Vibrio cholerae* (VCS), which produces a ganglioside profile similar to that of GD3S deletion (Fig. 1), protects against kainate-induced destruction of pyramidal neurons in the CA3 hippocampal subfield (Dhanushkodi & McDonald, 2011). VCS has also been shown to protect against neurodegeneration induced by 1-methyl-4-phenyl-1,2,3,6-tetrahydropyridine (MPTP; Schneider *et al.*, 2015).

In addition to the elimination of GD3, another beneficial effect of GD3S deletion is a compensatory increase in GM1 ganglioside (Ariga *et al.*, 2013; Bernardo *et al.*, 2009; Dhanushkodi & McDonald, 2011; Kawai *et al.*, 2001; Zhou *et al.*, 2011). Exogenous GM1 has been shown to inhibit aggregation of α-synuclein in vesicle cultures and prevent destruction of dopaminergic neurons in the SNc after MPTP exposure (Fazzini *et al.*, 1990; Hadjiconstantinou *et al.*, 1989; Martinez *et al.*, 2007). One mechanism by which GM1 exerts neurotrophic effects on dopaminergic neurons is by enhancing glial cell-line-derived neurotrophic factor (GDNF) signaling through the "rearranged during transcription" (RET) receptor tyrosine kinase and GDNF family receptor α1 (GFRα1) components of the GDNF receptor complex (Hadaczek *et al.*, 2015; Newburn *et al.*, 2014). GM1 has also been demonstrated to be effective in clinical studies with Parkinson's patients (Schneider, 1998; Schneider *et al.*, 1995, 2010, 2013).

Despite the promising effects of exogenous GM1, it poorly crosses the blood-brain barrier and requires repeated injections (Ledeen & Wu, 2007; Wu *et al.*, 2012). The present study was conducted to provide a proof-in-principle test of whether a genetic approach that chronically increases endogenous GM1 and eliminates GD3 would be neuroprotective in the MPTP model of Parkinson's disease. The typical MPTP regimens induce a "sledge-hammer" lesion that is uncharacteristic of the slow neurodegeneration of Parkinson's disease. In the present study we used a lower dose of MPTP administered more often, an approach that has been used successfully in non-human primates (Schneider, 1990; Schneider & Roeltgen, 1993; Schneider *et al.*, 1994a, b). Our hypothesis was that targeted deletion of GD3S would protect nigrostriatal dopaminergic neurons and prevent motor deficits associated with MPTP administration.

Methods

Subjects

Mice lacking the gene encoding GD3 synthase (ST8 α-*N*-acetyl-neuraminide α-2, 8-sialyltransferase 1; *St8sia1*) on a hybrid B6129F1 background (C57BL/6N;129S6/SvEvTac) were purchased from MMRRC (#000037-MU; Columbia, MO). Although this hybrid strain is seldom used for MPTP studies, our pilot data as well as a report by Rommelfanger et al. (2007) showed robust loss of striatal dopamine similar to that seen in inbred C57BL/6N mice. Because our primary purpose was to evaluate the effect of GD3S deletion on neuronal loss before moving to knock-down studies in inbred mice, we chose not to spend several years back-crossing the knockout mice to an inbred strain. Mice were bred in-house and genotyped by polymerase chain reaction and identified by subcutaneous radio-frequency tags. The effects of GD3S deletion are well-established, primarily the elimination of all b-series gangliosides. In addition, there is an increase in GM1 and an even greater increase in GD1a, as constitutively high levels of ganglioside are synthesized but converted to a-series instead of b-series (Fig. 1; Ariga *et al.*, 2013; Bernardo *et al.*, 2009; Kawai *et al.*, 2001; Zhou *et al.*, 2011). Hydrolysis of terminal α(2→3) sialic acid bonds on GD1a by membrane-bound sialidase may also contribute to increased GM1 levels in these mice. Subjects were 48 male mice, 24 GD3S+/+ and 24 GD3S−/− littermates generated from heterozygous matings, approximately 3 months old at the start of testing. Mice were housed five per cage in microisolator cages under standard conditions in an AALAC-approved vivarium, except for the 5 days during and 5 days following the MPTP injection regimens as described below. Food and water were freely available for the duration of the study, and the vivarium was maintained on a 12:12-h light:dark cycle with lights on at 6 am. All procedures were conducted during the light cycle. All experimental procedures were approved by the Institutional Animal Care and Use Committee and were conducted in accordance with NIH guidelines.

1-Methyl-4phenyl-1,2,3,6-tetrahydropyridine (MPTP)

MPTP HCl (#0896, lot 48K1861; Sigma-Aldrich, St. Louis, MO, USA) was dissolved in physiological (0.9%) saline at a concentration of 1.1 mg/ml free base (1.2892 mg/ml salt). Mice were given one injection of MPTP or saline per day for 5 consecutive days, three times, each separated by 21 days. This MPTP regimen was used in an attempt to better re-

capitulate the slow neurodegeneration of Parkinson's disease compared to the more typical 25 or 30 mg/kg regimens. Injections were administered subcutaneously at a volume of 10 ml/kg to achieve dose of 11 mg/kg body weight. The 11 mg/kg dose was chosen based on literature showing significant lesions and/or behavioral deficits induced by doses this low or lower (D'Astous *et al.*, 2006; Ding *et al.*, 2012; Goldberg *et al.*, 2012), and our own pilot data in four mice per group showing that five injections over 5 days reduced striatal dopamine 54% in wild-type mice but only 27% in GD3S knockouts. In order to ensure behavioral deficits at this low dose, we administered the 5-injection, low-dose MPTP regimen three separate times approximately 21 days apart. Each regimen was followed by assessment of motor function.

While receiving MPTP injections, mice were housed in disposable cages in a dedicated room under negative pressure to protect personnel from the aeration of the toxic MPP+ metabolites excreted in the urine and feces. The cages remained in the room for 5 days after the last injection, when mice were transferred to clean microisolator cages and returned to the vivarium. MPTP and associated hazardous waste were handled in strict accordance with the safety guidelines outlined by Przedborski et al. (2001), and all procedures were approved by the Institutional Biosafety Committee.

Behavior

Mice are particularly resistant to the effects of MPTP compared to non-human primates, and mouse strains vary widely in their sensitivity to the toxin (Blesa *et al.*, 2012). The present study was the first investigation of MPTP in GD3S knockout mice, and the effects of this particular dosing regimen or in the B6129S hybrid strain were not known. Because of this, we conducted a comprehensive battery of motor tests. Mice were first given a baseline locomotor activity session, then trained to perform the rotorod and horizontal beam tasks to ensure proficient pre-lesion performance. Mice were assigned to MPTP or saline groups based on pre-MPTP locomotor activity data, with the constraint that all mice within a cage were assigned to the same lesion condition to avoid adventitious exposure to aerated MPP+ within the cage. Thus the cages were stratified by the mean distance traveled in the activity monitor, and assigned sequentially to lesion groups. There were no differences between those assigned to the two lesion groups, no genotype difference, and no Genotype X Lesion interaction [F's < 1.31, p's > .26]. The behavioral assessments were conducted after each of the three MPTP regimens, during a 16-day period beginning the day after mice were removed from quarantine. Except for the force-plate actimeter, all tasks were conducted after each of the three MPTP injection regimens. All mice performed the tasks in the same order, as listed below. Although there is a learning curve for some sensorimotor tests, such as the rotorod, we expected the lesioned mice to have progressively worse behavior with each MPTP repetition on many of the tasks.

Locomotor activity—Mice were placed in commercially-available activity monitors (MED Associates, Inc., Georgia, VT, USA) for a 30-min session as previously described (Dhanushkodi *et al.*, 2013; Harrison *et al.*, 2010; Harrison *et al.*, 2008; Siesser *et al.*, 2006). The activity monitors measured 27×27 cm, with 16 infrared photocell beams equally

spaced in the x and y axes of the horizontal plane, 1 cm from the floor of the monitor. An additional vector of 16 photo beams was situated 5 cm above the floor to track rearing.

Motor function—A battery of motor tasks was conducted to measure balance, coordination, and agility, as previously described (Dhanushkodi & McDonald, 2011; Liu *et al.*, 1997; McDonald *et al.*, 2001; Norflus *et al.*, 1998; Sango *et al.*, 1996; Sango *et al.*, 1995). Most of the motor testing occurred following MPTP lesions, but mice were pre-trained on the rotorod and horizontal beam tasks to ensure proficient performance before the first MPTP administration. Balance and coordination were accessed using a Rotamex-5 rotorod (Columbus Instruments, Columbus, OH, USA). After a single practice trial, mice were trained for three trials per day for 15 consecutive days to balance on a rotating rod 3 cm in diameter. The rotation speed increased from 0 to 80 RPM over a 5-min period, incrementing 0.8 RPM every 3 s. If a mouse fell within 15 s it was given a second opportunity, but the latency on the second opportunity was recorded as the score regardless of the first score. In some cases mice would grasp the rod and rotate around with it. When this occurred, the time at which the first rotation occurred was recorded, and latency to fall or to the first rotation was the measure of interest. Mice were given an additional three trials per day following the first two MPTP regimens, and three trials per day for 3 days following the last regimen. For data analytic purposes, the nine sessions following the last regimen were averaged and analyzed with the others in a repeated-measures analysis.

The horizontal beam task required the mouse to traverse a 0.64-cm diameter, 81-cm-long beam elevated 40 cm above a blanket. Mice were motivated by a 25-W white light bulb at the starting platform, and reinforced with entry into a dark box on the other side of the beam. Mice were placed on the 5-cm^2 starting platform, and latency to initiate (all four paws on the beam), latency to traverse, and the number of paw slips were recorded. The sessions were video-recorded for scoring of foot slips. Mice were trained gradually, before the first MPTP administration, by placing them close to the dark box. Following entry into the box mice were re-placed on the bar at greater distances from the dark box, and required to traverse the remaining length of the bar. When mice reliably and quickly crossed the bar from the platform they were deemed trained and pre-MPTP trials were recorded. For analysis, trials on which the latency to leave the platform exceeded 10 s were assigned a score of 10 s; these trials were not scored for total latency or foot-slips.

On the block test, mice were placed on a clean acrylic block, 10×10 cm and 3 cm high. The latency to put its forepaws and then all four paws on the table were recorded. The sticker test is the standard test of MPTP-induced loss of fine motor skills (Dhanushkodi *et al.*, 2013). In this test, mice were gently restrained by the scruff and a 0.64-cm diameter sticker placed on the mouse's nose. They were then immediately placed into a clean tub cage free to move about. Normal mice will rapidly and reliably remove a sticker from the nose once it is detected. The latency to the first attempt to remove the sticker was recorded, as well as the latency to remove the sticker following the first attempt. Grip strength was measured using a commercially-available meter (Columbus Instrument, Columbus, OH). In this test, the subject was lowered by the base of the tail to the grid attached to the meter. Upon grasping the grid, the experimenter then pulled the tail gently but firmly, and with consistent force, until the mouse released the grid. The maximal force was recorded. Mice were given three

trials using all four limbs followed by three trials using forelimbs only. On the vertical screen test, mice were placed on a vertical section of hardware cloth. The amount of time to start moving and the latency to move all four paws were recorded.

Gait analysis—A DigiGait apparatus (Mouse Specifics, Inc., Framingham, MA) was used to assess gait parameters. Mice were placed individually on a motor-driven treadmill at 20 cm/s with a transparent treadmill belt in a small testing chamber. Mice that did not keep up with the treadmill speed were excluded from the analyses. A high-speed camera mounted below the belt captured digital video images of the underside of the mouse (80 frames/s). The frames were recorded using the Mouse Specifics DigiVideo software and data were analyzed by the DigiGait software. Figure 2 illustrates some of the measures collected by the DigiGait software. Additional measures included 1) step angle, the angle at the intersection of lines extending caudally from the long axes of the two hind paws; 2) paw angle, the angle at the intersection of a line extending caudally from long axis of each of the four paws and the direction of movement, and 3) paw area, the area of the paw that comes in contact with the belt. Most measures were averaged to create a single value for forepaws and a single value for hindpaws. The absolute values of the paw angles were summed.

Force-plate analysis—A force-plate actimeter (BASi, West Lafayette, IN, USA) was used to probe for tremor as well as to measure gait and locomotor activity as previously described (Fowler *et al.*, 2001, 2002; Fowler & Muma, 2015; McKerchar *et al.*, 2006). The FPA consists of a 42-cm^2 carbon fiber plate suspended on four force transducers, one in each corner. The plate is located within a clear acrylic box, and the entire apparatus is housed within a sound-attenuating chamber outfitted with a house light and a fan for ventilation. Mice were habituated to the apparatus in groups (one cage at a time), for 3 hours before receiving MPTP. Following the last MPTP session each mouse was given a 5-min session individually, and the computer tracked force variations 200 times per second. The forces exerted across all four force transducers per unit time were summed and normalized for body weight to produce a vertical-force time series for each mouse. Time series were then Fast Fourier Transformed (MATLAB, The Mathworks, Inc.,Natick, MA) into the frequency domain to yield power spectra. Spectra during bouts of low mobility were integrated (summed) across the 5 to 15 Hz frequency band. These integrated power values were averaged across low mobility bouts to produce a single measure of integrated power per mouse. Additional measures of "long runs" and "crossings" were scored with the aid of a scrolling graphics program, written in Visual Basic to extract gait parameters that are not included in the commercial software (Fowler *et al.*, 2017; Stanford *et al.*, 2015). Long runs refers to the number of runs for which gait data were calculated (runs had to be long, fast, straight, and continuous with well-formed force-time waveforms), and crossings were counted on the basis of being long and straight (by visual inspection) but not necessarily fast and not having well-formed rhythmic waveforms.

Histology and Immunohistochemistry

Mice were sacrificed 23–26 days following the last MPTP injection (2–5 days after the last day of behavioral testing). Food and water were freely available to the time of euthanasia. Mice whose brains were used for histology were perfused transcardially with ice-cold saline,

followed with 4% paraformaldehyde in 0.1 mM PBS, pH 7.4. Brains were removed and post-fixed overnight in the same fixative, then cryo-protected in graded sucrose solutions (10–30%) over several days. 40-μm coronal sections were taken through the rostral-caudal extent of the substantia nigra (Bregma 1.4 to −3.8), and striatum using a cryostat. For immunohistochemistry, free-floating sections were treated first with phosphate buffered saline (PBS) containing 20% methanol and 0.3% hydrogen peroxide for 30 min., and rinsed thoroughly in PBS. Sections were then incubated in 10% normal horse serum in PBS containing 0.1% Triton X-100 for 30 min. and incubated overnight at 4° C with the rabbit primary antibody (1:1000) targeting tyrosine hydroxylase (TH; #AB152, Millipore, Billerica, MA). Following incubation sections were rinsed three times in PBS, incubated for 1 h in a biotinylated goat anti-rabbit IgG (Vector Laboratories, Burlingame, CA), washed thrice, and treated with avidin–biotin complex (Vectastain Elite ABC kit, Vector Laboratories) for 1 h and visualized using diaminobenzidine. Sections were then mounted on slides and air-dried, but not cover-slipped, to allow subsequent staining with cresyl violet. Sections were re-hydrated through a graded series of ethanol solutions to ddH$_2$O, then stained for 8 min. with 0.1% cresyl violet acetate (#C5042, Sigma, St. Louis, MO). Sections were then dehydrated in an increasing series of ethanol and finally xylene. Sections through the SNc were used for stereology as described below. Optical density of TH-positive fibers and terminals in the striatum was quantified from 8 to 11 (mean 9.6) grey-scale sections per subject in four subjects per group, using the public domain software ImageJ (http://rsb.info.nih.gov/ij). An analysis of the entire visible striatum was made first, followed by a measurement of density in the dorsolateral striatal quadrant. Identical parameters were used for each measurement.

High-performance liquid chromatography (HPLC) with electrochemical detection

Mice used for neurochemistry were transported to the procedure room and remained undisturbed for 90 min. before being euthanized by cervical dislocation without anesthesia. All mice used for HPLC were euthanized between 9 am and noon. Brains were rapidly removed and a coronal section was taken from Bregma to 1.0 mm anterior to Bregma using a brain matrix. A tissue punch was used to extract a 1-mm diam. sample from the dorsolateral striatum of the left hemisphere, which was flash-frozen. Monoamines and their metabolites were measured from the 1-mm punches as previously described (Dhanushkodi *et al.*, 2013; Maiti *et al.*, 2016; Siesser *et al.*, 2006), in 12 mice per group. Briefly, the punches were suspended in 400-μl artificial cerebrospinal fluid and 600-μl 0.2 mM perchloric acid, homogenized for 30 s, and then centrifuged at 10,000 RPM for 15 min at 4° C. The supernatant was filtered through a nylon syringe filter (0.2 μm) and frozen at −80° C. Frozen samples (20 μl; 1:1 dilution with polished HPLC-grade water) were automatically injected by an ESA 542 refrigerated auto sampler (ESA, Inc., Waltham, MA) onto a 150 ± 2 mm ODS C18 column connected to an ESA model 580 HPLC pump. The mobile phase, containing 80 mM sodium dihydrogen phosphate monohydrate, 2.0 mM 1-octanesulfonic acid sodium salt, 100-μl/L triethylamine, 5 nM EDTA, and 10% acetonitrile, pH 3.0, was perfused at 0.25 ml/min. Monoamine levels were determined using an ESA 5041 high-sensitivity analytical cell, an ESA 5020 guard cell, and an ESA Coulochem II 5200A electrochemical detector at a potential of 220 mV with the current gain at 10 nA and the

guard cell at +350mV. Under these conditions, the limit of detection for dopamine was 100 fg per injection.

Unbiased stereology

For unbiased stereological quantification of TH-positive cells, neurons in every fourth section through the rostro-caudal extent of the substantia nigra pars compacta (SNc) were counted in 6–12 sections (mean 8.5) from four mice per group using the optical fractionator method and Stereo Investigator software (MBF Bioscience, Williston, VT) as previously described (Dhanushkodi *et al.*, 2013; Flanigan *et al.*, 2014; Maiti *et al.*, 2016). After delineation of the SNc at low magnification (4x objective), a point grid was overlaid onto each section. TH-positive cells were counted using a 60x objective. The grid size was chosen to achieve an average of 30 sampling sites per section. Gunderson coefficients (m=1) ranged from 0.04 to 0.09 (mean 0.059). The counting frames were selected using a systematic random sampling scheme, which provides an unbiased and efficient sampling technique. In every counting frame location, the top of the section was identified, after which the plane of the focus was moved 4 μm deeper through the section (guard zone) to prevent counting inaccuracies due to uneven section surfaces. The resulting focal plane served as the first point of the counting process, and TH-positive neurons that came into focus in the next 8-μm segment (dissector height) were counted if they were entirely within the 25 μm × 25 μm counting frame or intersecting the upper or right-side counting-frame boundaries. Based on the these parameters and counts, the total number of TH-positive cells per selected region were counted using the optical fractionator formula $N = 1/ssf \times 1/asf \times 1/hsf \times Q$, where ssf is the section sampling fraction, asf is the area sampling fraction, hsf is the height sampling fraction (dissector height divided by the section thickness after shrinkage), and Q denotes the total count of particles sampled for each region. After TH-positive neurons were counted, sections were counterstained with cresyl violet (CV) and all neurons that were CV+ but TH- were counted in an identical fashion.

Statistical analyses

All statistical analyses were performed using JMP Pro 12.0.1 (SAS Institute, Cary, NC, USA). Most behavioral, histological and neurochemical data were analyzed using two-way analysis of variance (ANOVA) or repeated-measures ANOVA (RMANOVA), with lesion (saline or MPTP) and genotype (GD3S+/+ or GD3S−/−) as between-subjects variables. Follow-up tests were conducted using orthogonal contrasts or Fisher's Protected LSD as appropriate. Heteroscedastic data were analyzed using Mann-Whitney U. Time-series data were analyzed using hierarchical linear modeling with subject as a random nominal variable nested within genotype and lesion, and time as a balanced continuous variable. Body weight differed across groups for the duration of the study, as detailed below. Because body weight has been shown to affect performance on the rotorod and other motor tasks, it was entered as a covariate in models assessing motor function after demonstration of homogeneity of regression slopes with genotype, lesion, and their interaction, and a linear relationship with the dependent measure of interest. The force-plate software contains internal controls for the subject's mass so a covariate was not needed for these data. All tests used an α level of 0.05 to determine statistical significance.

Results

Mice were weighed at the beginning of the study, and again before each MPTP injection regimen. There was a significant Time X Lesion group interaction across measurements [Fig. 3a; $F(3,129) = 3.6$, $p = .0164$]; main effects for genotype and lesion were not significant [F's < 2.6, p's > .118]. Follow-up contrasts showed that knockout mice in the saline group were heavier than those assigned to the MPTP group at the first measurement, i.e., before mice were actually assigned to lesion groups [$p = .0377$]. These same mice were significantly heavier at the third and fourth [p's < .0242] but not the second measurement [$p = .0701$]. There was no difference in body weight between the two wild-type groups at any time point [p's = .303]. Notably, although Fig. 3a refers to pre- and post-MPTP measurements, this terminology is to maintain parallelism with the behavioral assessments; the first two body weight measurements were taken before any administration of MPTP. Because of these group differences, body weight was used as a covariate in the analysis of motor tests that met the appropriate assumptions as noted above. Mice were pre-trained on the rotorod and horizontal bar tasks to ensure proficient performance before lesioning. There were no significant effects of genotype or lesion, or their interaction, on the rotorod test [F's < 2.3, p's > .140]. There were no group differences in latency to initiate, latency to cross, or total latency to traverse the 81-cm beam [F's < 4.1, p's > .052]. However, there was a significant genotype effect on the number of foot-slips [$F(1,43) = 7.4$, $p = .0094$]. Follow-up tests showed that knockout mice assigned to the saline group made significantly more foot slips per trial [0.42 ± 0.19] than their wild-type counterparts [0.00 ± 0.00; $p = .0403$]. The difference was not significant in mice assigned to receive MPTP [WT 0.17 ± 0.11 vs. KO 0.50 ± 0.15; $p = .091$].

Although the cumulative dose of MPTP was equivalent to 33 mg/kg over 5 days, sensorimotor performance on the standard battery of motor tasks was only mildly affected. Interaction effects were also largely non-significant, with the exception of habituation across sessions in the locomotor activity monitors and motor learning on the rotorod, equivalent in all groups. These data are presented in Table 1. In the force-plate actimeter, MPTP significantly impaired the two measures of long, continuous straight-line activity (runs & crossings) in wild-type mice only [p's < .0310]. There was no effect of MPTP on knockout mice, although even knockouts in the saline group had significantly lower scores on both measures than wild-type mice treated with saline [p's < .048]. There were parallel genotype effects on the conceptually-similar measures of total distance and bouts of low mobility [p's < .0200]. Additional force-plate data are presented in Table 2.

On the DigiGait apparatus there was a significant Genotype X Session interaction on forepaw stance width [$F(2,67) = 4.0$, $p = .0223$], reflecting slightly lower values on the part of the GD3S−/− saline group on the first session only [Fig. 3b; $p = .0016$]. All other group comparisons for this measure were non-significant on all sessions [p's > .313]. There were significant lesion effects on forepaw angle and forepaw area, and a significant Lesion X Session interaction on hindpaw stance width [F's > 3.8, p's < .027; Fig. 3c–d, Table 3]. Other effects were not significant [F's < 2.2, p's > .119]. The forepaw area effect was the result of larger paw areas in MPTP-lesioned mice in session 1 only [Fig. 3c; p's < .0473]. Comparisons at other time points for this measure were not significant [p's > .334]. The

significant interaction on hindpaw stance width reflected wider stances in MPTP-lesioned mice of both groups on session 3 [p = .0281] but not sessions 1 or 2 [Fig. 3d; p's > .090]. There were significant Genotype X Lesion X Session interactions on the hindpaw measures of swing, stride duration, stride length, and stride frequency [F's > 3.9, p's < .0242]. Main effects of genotype and lesion, and their interactions with session, were not significant for these measures [F's < 2.3, p's > .139]. The hindpaw swing effect reflected longer swings in MPTP-lesioned wild-type mice on the third session [Fig. 3e; p = .0066] but not the first two sessions [p's > .327]. MPTP did not affect GD3S−/− mice on any of the sessions [p's > .218]. Similarly, the hindpaw stride effect resulted from slower strides in wild-type mice given MPTP, compared to their saline-treated counterparts [Fig. 3f; p = .035]. Stride length and frequency are variants of stride duration, and results were similar for those measures except that the 3rd-session difference between MPTP- and saline-treated wild-type mice was significant for stride length [p = .032] but not frequency [p = .072]. Additional gait data are presented in Table 3.

Following the last session of behavioral testing, mice were euthanized and brains processed for immunohistochemistry or HPLC. MPTP induced a significant reduction in striatal dopamine [Table 4; F(1,41) = 31.6, p < .0001]. Genotype and Genotype X Lesion interaction effects were not significant [p's > .154]. Follow-up comparisons by genotype showed that the lesion effect was significant in both wild-type and knockout mice [p's < .003], although the magnitude of dopamine loss was larger in wild-type mice (60.7 ± 5.1%) than in knockouts (37.2 ± 8.0%). There were no main or interaction effect on HVA levels [F's < 3.1, p's > .087], but there was a significant lesion effect on DOPAC [F(1,41) = 13.9, p = .0006] and a significant Genotype X Lesion interaction for 3-MT [F(1,41) = 4.1, p = .0492]. Follow-up comparisons showed that DOPAC levels were decreased significantly by MPTP in mice of both genotypes [p's <.018], but that 3-MT was reduced in the wild-type mice [p = .0282] but not in the knockouts [p = .570]. There were no significant effects on DOPAC/DA [F's < 1.4, p's > .256]; however, there was a significant lesion effect on HVA/DA [F(1,41) = 25.9, p < .0001] and significant genotype and lesion effects on 3-MT/DA [F's > 7.8, p's <.008]. Follow-up comparisons showed that the lesion effects on HVA/DA and 3-MT/DA were significant in both genotypes [p's < .041]. The genotype effect on 3-MT/DA was significant in MPTP-lesioned mice [p = .0406] but not in saline-treated controls [p = .0725], although the magnitude of the effect was similar for both comparisons (saline 24.4 ± 5.4% vs. MPTP 19.4 ± 7.4%). There were no significant genotype or lesion effects on striatal NE [F's < 1.7, p's > .213]. There was a significant lesion effect on DHPG [F(1,23) = 4.7, p = .0418], but no group differences on follow-up [p's > .053]. Main and interaction effects for DHPG/NE were not significant [F's < 0.5, p's > .478]. There was a significant lesion effect on DA/NE [F(1,40) = 11.7, p = .0015]. Follow-up comparisons showed that the lesion effect on DA/NE was significant in both genotypes [p's < .03]. There was a significant genotype effect on 5-HT [F(1,41) = 4.2, p = .0459]. Lesion and interaction effects were not significant [F's < 0.1, p's > .724]. There were no main or interaction effects on 5-HIAA [F's < .8, p's > .387], but there was a significant genotype effect on 5-HIAA/5-HT [F(1,41) = 6.7, p = .0135]. 5-HT was 46.1 ± 20.0% higher in GD3S−/− mice compared to wild-type controls, but the difference was not statistically significant in either lesion group on follow-up [p's > .098]. The genotype effect on 5-HIAA/5-HT was significant in MPTP-

lesioned mice [p = .0395] but not saline-treated controls [p = .137] although, as with 3-MT/DA, the magnitude of the differences was similar (saline 17.1 ± 9.1% vs. MPTP 23.6 ± 5.2%). All monoamine data are summarized in Table 3.

Following three regimens of 11 mg/kg MPTP there was a significant reduction in the TH-positive cell count [Fig. 4; F(1,12) = 9.3, p = .0101]. Follow-up comparisons showed that TH-positive cell count was significantly reduced by MPTP in the wild-type [p = .0109] but not in the knockout mice [p = .2174], indicating that both genotypes were not affected equally by the neurotoxin. The difference between wild-type and GD3S−/− MPTP-lesioned groups was not significant [p=.1185]. Interestingly, counterstaining with cresyl violet (CV) also revealed a significant lesion effect on the count of CV-positive neurons that were negative for TH [Fig 4f; F(1,12) = 6.1, p = 0.0294]. Follow-up analysis showed that CV-positive cell count was significantly higher only in knockouts [p = .0205] but not in wild-types [p = .4244] lesioned with MPTP when each group was compared with its own saline-treated controls. When TH+ and CV+ neurons were summed (Fig. 4g), there were significant main effects for genotype and lesion [F's > 4.7, p's < .0492]. Follow-up comparisons showed that total neuron number in wild-type mice lesioned with MPTP was significantly reduced [p = .0114], but was unchanged by MPTP in GD3S−/− mice [p = .803]. Densitometry was used to analyze the optical density of TH-positive fibers in whole striatum as well as the dorsolateral quadrant for possible differences in neuroprotection. There was a significant genotype effect on optical density in striatum [Fig. 5; F(1,12) = 8.5, p = .013]. Follow-up comparisons showed that the optical density in striatum was significantly reduced in the wild-type mice [p = .0271] but not in the knockout mice [p = .6983]. Figure 5i shows that TH-positive optical density was reduced 19.0 ± 2.5% in the wild-type mice lesioned with MPTP, consistent with the SNc lesion observed in Figure 4. None of the omnibus or follow-up tests was significant when the dorsolateral quadrant was considered [F's < 3.4, p's > .091]. However, a non-significant loss of TH-positive fibers 14.7 ± 3.1% was observed in the wild-type mice treated with MPTP (Fig. 5j).

Discussion

We show here that deletion of GD3S affords neuroprotection against MPTP neurotoxicity, and a corresponding protection against loss of striatal dopamine. The low-dose regimen used did not produce robust behavioral impairments, although with the more sensitive force-plate and gait-analysis apparatus we were able to detect MPTP-induced deficits. Some previously-unknown reductions in locomotor activity were detected in GD3S−/− mice, and some MPTP-induced deficits were absent in the knockouts. Consistent with our previous studies, these data suggest that interventions that simultaneously decrease GD3 and increase endogenous GM1 can be neuroprotective.

The purpose of using the extended low-dose MPTP regimen in the present study was to attempt to better recapitulate the slow neurodegeneration of Parkinson's disease. Our mice received a cumulative dose of 165 mg/kg (11 mg/kg x 5 days x 3 regimens). This is somewhat higher than the typical subchronic regimen of five injections of 25 or 30 mg/kg. Nevertheless, we observed smaller SNc lesions and virtually no MPTP effects on the standard assessment of Parkinsonism. In our hands, a 5-day regimen of 18 mg/kg of the

same lot of MPTP destroyed 41% and 45% of the TH+ SNc neurons in control animals, and 25 mg/kg produced a lesion sizes of 75% and 79% (Dhanushkodi *et al.*, 2013; Maiti *et al.*, 2016; and unpublished data). The regimen in the present study produced a smaller lesion (53%) than the 25 mg/kg dose. Large lesion sizes are typically needed to observe behavioral effects of MPTP, although we saw mild deficits in the present study and with the 18 mg/kg dose (Dhanushkodi *et al.*, 2013). The lack of robust behavioral changes may be attributable to the lower absolute dose and/or to the functional recovery that takes place following MPTP lesioning. Indeed, the sprouting and regeneration of new dopaminergic fibers, accompanied by functional recovery, is a well-established phenomenon that has been shown to begin within 24 hours of the last injection (Bezard *et al.*, 2000a; Bezard & Gross, 1998; Bezard *et al.*, 2000b; Bohn *et al.*, 1988; Domenger *et al.*, 2012; Kang *et al.*, 2007; Mitsumoto *et al.*, 1998; Schneider & Yuwiler, 1989).

Strain differences may also be a factor in the MPTP response. The GD3S−/− mice are on a hybrid C57BL/6J + 129S6/SvEvTac background, whereas our previous studies used the C57BL/6N inbred strain. To our knowledge the low-dose regimen used in the present study has not been published before, so it is impossible to know what size lesion would be produced in the C57BL/6N strain or other C57BL/6 substrains. Considerable evidence shows sizeable behavioral and catecholaminergic differences among 129/Sv and C57BL/6 inbred strains and their hybrids (Bothe *et al.*, 2005; He & Shippenberg, 2000; Hughes, 1989; Kelly *et al.*, 1998; McCutcheon *et al.*, 2008; Montkowski *et al.*, 1997; Wolfer *et al.*, 1997). Indeed, an analysis of recombinant inbred strains showed that response to MPTP is a multigenic trait (Jones *et al.*, 2013). In that study the reduction in striatal TH ranged from 20–75% across 10 strains. The strain differences were even greater in the dopamine metabolites DOPAC, HVA, and 3-MT and their estimates of dopamine turnover, with some higher and some lower than saline controls. This may explain why we observed the typical MPTP-induced increases in HVA/DA and 3-MT/DA in wild-type mice but a smaller, non-significant increase in DOPAC/DA. Increases in these estimates of dopamine turnover are expected following MPTP, but with strain and methodological differences the nature of the changes can vary from study to study. However, the focus of the present study was to determine the neuroprotective effects of GD3S deletion, and the availability of the knockout mice restricted the choice of background. Thus, although there may be several reasons why robust behavioral effects were not detected in wild-type mice in the present study, the neuroprotective effects of knocking out GD3S were clear.

In the force-plate analysis, MPTP reduced activity in wild-type mice. This could not be compared directly to the GD3S−/− mice because both saline- and MPTP-treated knockout groups also had reduced activity (Table 1). Several papers reported that GD3S knockouts on mixed or unspecified backgrounds had no obvious neurological abnormalities and normal morphology and conduction velocity in the spinal cord and sciatic nerve (Bernardo *et al.*, 2009; Handa *et al.*, 2005; Kawai *et al.*, 2001). However, a more recent study documented sciatic dysmorphology in GD3S−/− mice on an inbred 129/SvEv background (Ribeiro-Resende *et al.*, 2014). This report shows that GD3S plays a role in nerve integrity and its absence may result in motor deficits.

MPTP also altered gait parameters in the present study. Wild-type, but not GD3S−/− mice, exhibited longer hindpaw swing and stride durations following the last MPTP regimen (Fig. 3e,f). The literature is mixed with respect to the effects of MPTP on stride duration in mice. In C57BL/6 substrains subchronic MPTP typically shortens strides or has no effect, with belt speeds ranging from 20 to 34 cm/s or on a stationery runway. The critical factor may be the daily dose. Doses ranging from 5 to 15 mg/kg produced no stride alterations (Antzoulatos *et al.*, 2010; Byler *et al.*, 2009; Guillot *et al.*, 2008), whereas 20 mg/kg or higher resulted in shorter strides (Amende *et al.*, 2005; Fernagut *et al.*, 2002; Goldberg *et al.*, 2011; Guillot *et al.*, 2008; Samantaray *et al.*, 2015; Wang *et al.*, 2012; Zhao *et al.*, 2010, 2013). The notable exception is Feng et al. (2014), who reported longer stride durations in C57BL/6J mice after 7 injections of 30 mg/kg/day. We are only aware of a single MPTP study performed using B6129 mice (Rommelfanger *et al.*, 2007). In that study, strides were increased 13% in control mice after two administrations of 30 mg/kg MPTP 12 h apart. Interestingly, two non-MPTP studies using B6129 hybrids also showed longer strides in mouse models of autism (Piochon *et al.*, 2015) and Alzheimer's disease (Stover *et al.*, 2015). A systematic study would be required to determine whether strain, low absolute dose (11 mg/kg), or other factors contributed to the longer strides in the present study. However, the effects were only evident after the third MPTP regimen and only in wild-type mice. This suggests that a threshold lesion size may be necessary for MPTP-induced gait disturbances, which was not met in GD3S−/− mice.

The relatively mild behavioral effects of MPTP in wild-type mice are perhaps surprising given the nearly 60% loss of striatal dopamine. The loss of dopamine was considerably less in knockout mice. TH-positive neurons in the SNc exhibited a similar degree of neuroprotection in MPTP-lesioned GD3S−/− mice, and TH fiber density in the striatum was equivalent to that of saline-treated controls. Interestingly, the number of CV-stained neurons in the SNc that were negative for TH was greater in MPTP-lesioned knockout mice than in saline-treated controls (Fig. 4b). This phenomenon has been reported previously—specifically, a suppression of TH in surviving dopaminergic neurons after lesioning with MPTP or 6-hydroxydopamine (6-OHDA; Bowenkamp *et al.*, 1996a, 1996b; Georgievska *et al.*, 2002; Jackson-Lewis *et al.*, 1995; Porritt *et al.*, 2005; Rosenblad *et al.*, 2003; Sauer & Oertel, 1994; Smith *et al.*, 2011). The mechanism for this is not known, but may involve elevated neurotrophin signaling. Georgievska et al. (2002) showed that locally-high concentrations of GDNF suppressed TH expression for 3–6 weeks after intrastriatal GDNF injections in rats with 6-OHDA lesions. In areas along the nigro-striatal pathway that had lower GDNF, TH was normally expressed in surviving neurons. This is consistent with other papers showing normal TH expression when local GDNF concentrations were 5–10 times lower (Kirik *et al.*, 2000; Kordower *et al.*, 2000). It is not known how TH suppression is related to GDNF-mediated neuroprotection following MPTP or 6-OHDA. Cohen et al. (2011) proposed that in the presence of neurotoxin GDNF temporarily induces a shift in the cell's state to a "maintenance mode", which includes down-regulation of TH. Once the neuron's survival is ensured, normal cellular functions are restored. The TH suppression is maximal at approximately 2 weeks following MPTP injections, and returns to normal by 8 weeks (Cohen *et al.*, 2011; Sauer & Oertel, 1994). There is reason to suspect that this may have happened in the GD3S−/− mice. It is well-established that knocking out GD3S results

in a compensatory increase in GM1 ganglioside in addition to eliminating all b-series gangliosides (Ariga *et al.*, 2013; Bernardo *et al.*, 2009; Dhanushkodi & McDonald, 2011; Kawai *et al.*, 2001; Zhou *et al.*, 2011). GDNF is required for survival of dopaminergic neurons, and GM1 is important for proper GDNF signaling (Hadaczek *et al.*, 2015). GM1 associates with the GFRα1 and RET components of the tripartite GDNF receptor and is required for its assembly (Hadaczek *et al.*, 2015; Newburn *et al.*, 2014). Mice null for *B4galnt1*, the gene that codes for GalNAc transferase (Fig. 1), completely lack GM1 and exhibit profound age-related motor impairments and loss of TH+ staining in the SNc (Wu *et al.*, 2011). They also have impaired GDNF signaling secondary to insufficient RET phosphorylation (Hadaczek *et al.*, 2015). Brain GM1 is reduced by about 15% in young *B4galnt1*+/− mice, a deficit that increases to ~50% in mice older than 6 months of age (Wu *et al.*, 2012). The heterozygous mice have a longer life span than the homozygotes but the same profound age-related Parkinsonism and nigrostriatal pathology. SNc TH expression in the *B4galnt1* heterozygotes can be reversed with several weeks of injections of exogenous GM1 or LIGA-20, a synthetic GM1 analog. This demonstrates that the neurons are alive but just not expressing TH. We can't say definitively why there were more CV+/TH- neurons in GD3S knockout mice treated with MPTP in the present study. However, the total number of TH+ and CV+ neurons in the GD3S−/− mice treated with MPTP is approximately the same number as that in the two saline-treated groups (Fig. 4g). Thus it appears that deletion of GD3S afforded full protection of SNc neurons but that TH expression was suppressed in a subset of them. Further investigation is needed to determine the long-term fate of these neurons and potential reasons for suppression of TH.

The requirement for *de novo*-synthesized GD3 in apoptotic pathways is well-established (De Maria *et al.*, 1997; De Maria *et al.*, 1998; Melchiorri *et al.*, 2002; Morales *et al.*, 2004), as is the literature showing neuroprotective effects of exogenous GM1 and manipulations that enhance endogenous GM1; in contrast, neurodegeneration is exacerbated neurodegeneration in animals with reduced GM1 (Ariga *et al.*, 2013; Bernardo *et al.*, 2009; Dhanushkodi & McDonald, 2011; Hadaczek *et al.*, 2015; Wu *et al.*, 2012; Yao *et al.*, 2014). Thus our first inclination is to attribute the neuroprotective effect of GD3S deletion to the lack of GD3 and/or increased GM1. The phenotype of the *B4galnt1*+/− mice suggests that the change in GM1 may be the more important mechanism of the two. The SNc pathology was completely reversed by administration of GM1 to the *B4galnt1* heterozygotes, and they exhibited no substantive neuronal loss despite more than 10-fold higher levels of GD3 (Liu *et al.*, 1999; Wu *et al.*, 2001; Zhou *et al.*, 2011). However, other factors may also affect the sensitivity of GD3S−/− mice to MPTP, such as the lack of b-series gangliosides in the knockouts. Although there is considerable functional overlap across gangliosides, and total ganglioside levels are unchanged in GD3S−/− mice, we do not know how lacking b-series gangliosides affects nigrostriatal function or response to MPTP independent of changes in GD3 and GM1. Other neurochemical changes may also be involved, such as the ~20% reduction in 5-HIAA/5-HT observed in GD3S knockout mice. Serotonin transporter knockout mice have a reduced locomotor response to amphetamine (Igari *et al.*, 2015), and the serotonin transporter is required for expression of cocaine place preference in mice lacking the dopamine transporter (Sora *et al.*, 2001). Like cocaine and amphetamine, MPTP's active metabolite MPP+ acts through the dopamine transporter, and reduced serotonin turnover

may have affected its neurotoxicity. Further research is needed to determine whether these or other neurochemical mechanisms interact with ganglioside alterations to modify the neuroprotective effect of GD3S deletion.

Acknowledgments

References

Abbott SK, Li H, Munoz SS, Knoch B, Batterham M, Murphy KE, Halliday GM, Garner B. Altered ceramide acyl chain length and ceramide synthase gene expression in Parkinson's disease. Mov Disord. 2014; 29:518–526. [PubMed: 24822250]

Amende I, Kale A, McCue S, Glazier S, Morgan JP, Hampton TG. Gait dynamics in mouse models of Parkinson's disease and Huntington's disease. Journal of neuroengineering and rehabilitation. 2005; 2:20. [PubMed: 16042805]

Anglade P, Vyas S, Javoy-Agid F, Herrero MT, Michel PP, Marquez J, Mouatt-Prigent A, Ruberg M, Hirsch EC, Agid Y. Apoptosis and autophagy in nigral neurons of patients with Parkinson's disease. Histol Histopathol. 1997; 12:25–31. [PubMed: 9046040]

Antzoulatos E, Jakowec MW, Petzinger GM, Wood RI. Sex differences in motor behavior in the MPTP mouse model of Parkinson's disease. Pharmacol Biochem Behav. 2010; 95:466–472. [PubMed: 20347863]

Ariga T, Itokazu Y, McDonald MP, Hirabayashi Y, Ando S, Yu RK. Brain gangliosides of a transgenic mouse model of Alzheimer's disease with deficiency in GD3-synthase: expression of elevated levels of a cholinergic-specific ganglioside, GT1aα. ASN Neuro. 2013; 5:141–148. [PubMed: 23565921]

Ariga T, Jarvis WD, Yu RK. Role of sphingolipid-mediated cell death in neurodegenerative diseases. J Lipid Res. 1998; 39:1–16. [PubMed: 9469581]

Bernardo A, Harrison FE, McCord M, Zhao J, Bruchey A, Davies SS, Jackson Roberts L 2nd, Mathews PM, Matsuoka Y, Ariga T, Yu RK, Thompson R, McDonald MP. Elimination of GD3 synthase improves memory and reduces amyloid-β plaque load in transgenic mice. Neurobiol Aging. 2009; 30:1777–1791. [PubMed: 18258340]

Bernheimer H, Birkmayer W, Hornykiewicz O, Jellinger K, Seitelberger F. Brain dopamine and the syndromes of Parkinson and Huntington. Clinical, morphological and neurochemical correlations. J Neurol Sci. 1973; 20:415–455. [PubMed: 4272516]

Bezard E, Dovero S, Imbert C, Boraud T, Gross CE. Spontaneous long-term compensatory dopaminergic sprouting in MPTP-treated mice. Synapse. 2000a; 38:363–368. [PubMed: 11020240]

Bezard E, Gross CE. Compensatory mechanisms in experimental and human parkinsonism: towards a dynamic approach. Prog Neurobiol. 1998; 55:93–116. [PubMed: 9618745]

Bezard E, Jaber M, Gonon F, Boireau A, Bloch B, Gross CE. Adaptive changes in the nigrostriatal pathway in response to increased 1-methyl-4-phenyl-1,2,3,6-tetrahydropyridine-induced neurodegeneration in the mouse. Eur J Neurosci. 2000b; 12:2892–2900. [PubMed: 10971632]

Blesa J, Phani S, Jackson-Lewis V, Przedborski S. Classic and new animal models of Parkinson's disease. J Biomed Biotechnol. 2012; 2012:845618. [PubMed: 22536024]

Bohn MC, Marciano F, Cupit L, Gash DM. Recovery of dopaminergic fibers in striatum of the 1-methyl-4-phenyl-1,2,3,6-tetrahydropyridine-treated mouse is enhanced by grafts of adrenal medulla. Prog Brain Res. 1988; 78:535–542. [PubMed: 3266803]

Bothe GW, Bolivar VJ, Vedder MJ, Geistfeld JG. Behavioral differences among fourteen inbred mouse strains commonly used as disease models. Comp Med. 2005; 55:326–334. [PubMed: 16158908]

Bowenkamp KE, David D, Lapchak PL, Henry MA, Granholm AC, Hoffer BJ, Mahalik TJ. 6-hydroxydopamine induces the loss of the dopaminergic phenotype in substantia nigra neurons of the rat. A possible mechanism for restoration of the nigrostriatal circuit mediated by glial cell line-derived neurotrophic factor. Exp Brain Res. 1996a; 111:1–7. [PubMed: 8891630]

Bowenkamp KE, Lapchak PA, Hoffer BJ, Bickford PC. Glial cell line-derived neurotrophic factor reverses motor impairment in 16–17 month old rats. Neurosci Lett. 1996b; 211:81–84. [PubMed: 8830849]

Brugg B, Michel PP, Agid Y, Ruberg M. Ceramide induces apoptosis in cultured mesencephalic neurons. J Neurochem. 1996; 66:733–739. [PubMed: 8592146]

Byler SL, Boehm GW, Karp JD, Kohman RA, Tarr AJ, Schallert T, Barth TM. Systemic lipopolysaccharide plus MPTP as a model of dopamine loss and gait instability in C57Bl/6J mice. Behav Brain Res. 2009; 198:434–439. [PubMed: 19070633]

Cohen AD, Zigmond MJ, Smith AD. Effects of intrastriatal GDNF on the response of dopamine neurons to 6-hydroxydopamine: time course of protection and neurorestoration. Brain Res. 2011; 1370:80–88. [PubMed: 21062624]

Connolly BS, Lang AE. Pharmacological treatment of Parkinson disease: a review. JAMA. 2014; 311:1670–1683.

D'Astous M, Mendez P, Morissette M, Garcia-Segura LM, Di Paolo T. Implication of the phosphatidylinositol-3 kinase/protein kinase B signaling pathway in the neuroprotective effect of estradiol in the striatum of 1-methyl-4-phenyl-1,2,3,6-tetrahydropyridine mice. Mol Pharmacol. 2006; 69:1492–1498. [PubMed: 16434614]

De Maria R, Lenti L, Malisan F, d'Agostino F, Tomassini B, Zeuner A, Rippo MR, Testi R. Requirement for GD3 ganglioside in CD95- and ceramide-induced apoptosis. Science. 1997; 277:1652–1655. [PubMed: 9287216]

De Maria R, Rippo MR, Schuchman EH, Testi R. Acidic sphingomyelinase (ASM) is necessary for fas-induced GD3 ganglioside accumulation and efficient apoptosis of lymphoid cells. J Exp Med. 1998; 187:897–902. [PubMed: 9500792]

Dhanushkodi A, Akano EO, Roguski EE, Xue Y, Rao SK, Matta SG, Rex TS, McDonald MP. A single intramuscular injection of rAAV-mediated mutant erythropoietin protects against MPTP-induced parkinsonism. Genes, brain, and behavior. 2013; 12:224–233.

Dhanushkodi A, McDonald MP. Intracranial *V. cholerae* sialidase protects against excitotoxic neurodegeneration. PLoS One. 2011; 6:e29285. [PubMed: 22195039]

Ding H, Wang Q, Liu J, Qian W, Wang W, Wang J, Gao R, Xiao H. Alterations of gene expression of sodium channels in dorsal root ganglion neurons of estrogen receptor knockout (ERKO) mice induced by 1-methyl-4-phenyl-1,2,3,6-tetrahydropyridine (MPTP). Endocrine. 2012; 42:118–124. [PubMed: 22371119]

Domenger D, Dea D, Theroux L, Moquin L, Gratton A, Poirier J. The MPTP neurotoxic lesion model of Parkinson's disease activates the apolipoprotein E cascade in the mouse brain. Exp Neurol. 2012; 233:513–522. [PubMed: 22155743]

Fazzini E, Durso R, Davoudi H, Szabo GK, Albert ML. GM1 gangliosides alter acute MPTP-induced behavioral and neurochemical toxicity in mice. J Neurol Sci. 1990; 99:59–68. [PubMed: 2250172]

Feng G, Zhang Z, Bao Q, Zhang Z, Zhou L, Jiang J, Li S. Protective effect of chinonin in MPTP-induced C57BL/6 mouse model of Parkinson's disease. Biol Pharm Bull. 2014; 37:1301–1307. [PubMed: 24871044]

Fernagut PO, Diguet E, Labattu B, Tison F. A simple method to measure stride length as an index of nigrostriatal dysfunction in mice. J Neurosci Methods. 2002; 113:123–130. [PubMed: 11772434]

Flanigan TJ, Xue Y, Kishan Rao S, Dhanushkodi A, McDonald MP. Abnormal vibrissa-related behavior and loss of barrel field inhibitory neurons in 5xFAD transgenics. Genes, brain, and behavior. 2014; 13:488–500.

Forno LS, Sternberger LA, Sternberger NH, Strefling AM, Swanson K, Eng LF. Reaction of Lewy bodies with antibodies to phosphorylated and non-phosphorylated neurofilaments. Neurosci Lett. 1986; 64:253–258. [PubMed: 2421208]

Fowler SC, Birkestrand BR, Chen R, Moss SJ, Vorontsova E, Wang G, Zarcone TJ. A force-plate actometer for quantitating rodent behaviors: illustrative data on locomotion, rotation, spatial

patterning, stereotypies, and tremor. J Neurosci Methods. 2001; 107:107–124. [PubMed: 11389948]

Fowler SC, Mosher LJ, Godar SC, Bortolato M. Assessment of gait and sensorimotor deficits in the D1CT-7 mouse model of Tourette syndrome. J Neurosci Methods. 2017

Fowler SC, Muma NA. Use of a force-sensing automated open field apparatus in a longitudinal study of multiple behavioral deficits in CAG140 Huntington's disease model mice. Behav Brain Res. 2015; 294:7–16. [PubMed: 26210937]

Fowler SC, Zarcone TJ, Vorontsova E, Chen R. Motor and associative deficits in D2 dopamine receptor knockout mice. International journal of developmental neuroscience : the official journal of the International Society for Developmental Neuroscience. 2002; 20:309–321. [PubMed: 12175868]

Georgievska B, Kirik D, Bjorklund A. Aberrant sprouting and downregulation of tyrosine hydroxylase in lesioned nigrostriatal dopamine neurons induced by long-lasting overexpression of glial cell line derived neurotrophic factor in the striatum by lentiviral gene transfer. Exp Neurol. 2002; 177:461– 474. [PubMed: 12429192]

Goldberg NR, Fields V, Pflibsen L, Salvatore MF, Meshul CK. Social enrichment attenuates nigrostriatal lesioning and reverses motor impairment in a progressive 1-methyl-2-phenyl-1,2,3,6-tetrahydropyridine (MPTP) mouse model of Parkinson's disease. Neurobiol Dis. 2012; 45:1051– 1067. [PubMed: 22198503]

Goldberg NR, Hampton T, McCue S, Kale A, Meshul CK. Profiling changes in gait dynamics resulting from progressive 1-methyl-4-phenyl-1,2,3,6-tetrahydropyridine-induced nigrostriatal lesioning. J Neurosci Res. 2011; 89:1698–1706. [PubMed: 21748776]

Guillot TS, Asress SA, Richardson JR, Glass JD, Miller GW. Treadmill gait analysis does not detect motor deficits in animal models of Parkinson's disease or amyotrophic lateral sclerosis. Journal of motor behavior. 2008; 40:568–577. [PubMed: 18980909]

Hadaczek P, Wu G, Sharma N, Ciesielska A, Bankiewicz K, Davidow AL, Lu ZH, Forsayeth J, Ledeen RW. GDNF signaling implemented by GM1 ganglioside; failure in Parkinson's disease and GM1-deficient murine model. Exp Neurol. 2015; 263:177–189. [PubMed: 25448159]

Hadjiconstantinou M, Mariani AP, Neff NH. GM1 ganglioside-induced recovery of nigrostriatal dopaminergic neurons after MPTP: an immunohistochemical study. Brain Res. 1989; 484:297– 303. [PubMed: 2565752]

Handa Y, Ozaki N, Honda T, Furukawa K, Tomita Y, Inoue M, Furukawa K, Okada M, Sugiura Y. GD3 synthase gene knockout mice exhibit thermal hyperalgesia and mechanical allodynia but decreased response to formalin-induced prolonged noxious stimulation. Pain. 2005; 117:271–279. [PubMed: 16150545]

Harrison FE, May JM, McDonald MP. Vitamin C deficiency increases basal exploratory activity but decreases scopolamine-induced activity in APP/PSEN1 transgenic mice. Pharmacol Biochem Behav. 2010; 94:543–552. [PubMed: 19941887]

Harrison FE, Yu SS, Van Den Bossche KL, Li L, May JM, McDonald MP. Elevated oxidative stress and sensorimotor deficits but normal cognition in mice that cannot synthesize ascorbic acid. J Neurochem. 2008; 106:1198–1208. [PubMed: 18466336]

He M, Shippenberg TS. Strain differences in basal and cocaine-evoked dopamine dynamics in mouse striatum. J Pharmacol Exp Ther. 2000; 293:121–127. [PubMed: 10734161]

Hughes AL. Interaction between strains in the social relations of inbred mice. Behav Genet. 1989; 19:685–700. [PubMed: 2803188]

Igari M, Shen HW, Hagino Y, Fukushima S, Kasahara Y, Lesch KP, Murphy DL, Hall FS, Uhl GR, Ikeda K, Yaegashi N, Sora I. Attenuated methamphetamine-induced locomotor sensitization in serotonin transporter knockout mice is restored by serotonin 1B receptor antagonist treatment. Behav Pharmacol. 2015; 26:167–179. [PubMed: 25485646]

Jackson-Lewis V, Jakowec M, Burke RE, Przedborski S. Time course and morphology of dopaminergic neuronal death caused by the neurotoxin 1-methyl-4-phenyl-1,2,3,6-tetrahydropyridine. Neurodegeneration. 1995; 4:257–269. [PubMed: 8581558]

Jones BC, Miller DB, O'Callaghan JP, Lu L, Unger EL, Alam G, Williams RW. Systems analysis of genetic variation in MPTP neurotoxicity in mice. Neurotoxicology. 2013; 37:26–34. [PubMed: 23558233]

Kang JM, Park HJ, Choi YG, Choe IH, Park JH, Kim YS, Lim S. Acupuncture inhibits microglial activation and inflammatory events in the MPTP-induced mouse model. Brain Res. 2007; 1131:211–219. [PubMed: 17173870]

Kawai H, Allende ML, Wada R, Kono M, Sango K, Deng C, Miyakawa T, Crawley JN, Werth N, Bierfreund U, Sandhoff K, Proia RL. Mice expressing only monosialoganglioside GM3 exhibit lethal audiogenic seizures. J Biol Chem. 2001; 276:6885–6888. [PubMed: 11133999]

Kelly MA, Rubinstein M, Phillips TJ, Lessov CN, Burkhart-Kasch S, Zhang G, Bunzow JR, Fang Y, Gerhardt GA, Grandy DK, Low MJ. Locomotor activity in D2 dopamine receptor-deficient mice is determined by gene dosage, genetic background, and developmental adaptations. J Neurosci. 1998; 18:3470–3479. [PubMed: 9547254]

Kirik D, Rosenblad C, Bjorklund A, Mandel RJ. Long-term rAAV-mediated gene transfer of GDNF in the rat Parkinson's model: intrastriatal but not intranigral transduction promotes functional regeneration in the lesioned nigrostriatal system. J Neurosci. 2000; 20:4686–4700. [PubMed: 10844038]

Kordower JH, Emborg ME, Bloch J, Ma SY, Chu Y, Leventhal L, McBride J, Chen EY, Palfi S, Roitberg BZ, Brown WD, Holden JE, Pyzalski R, Taylor MD, Carvey P, Ling Z, Trono D, Hantraye P, Deglon N, Aebischer P. Neurodegeneration prevented by lentiviral vector delivery of GDNF in primate models of Parkinson's disease. Science. 2000; 290:767–773. [PubMed: 11052933]

Ledeen R, Wu G. GM1 in the nuclear envelope regulates nuclear calcium through association with a nuclear sodium-calcium exchanger. J Neurochem. 2007; 103(Suppl 1):126–134. [PubMed: 17986147]

Liu Y, Hoffmann A, Grinberg A, Westphal H, McDonald MP, Miller KM, Crawley JN, Sandhoff K, Suzuki K, Proia RL. Mouse model of GM2 activator deficiency manifests cerebellar pathology and motor impairment. Proc Natl Acad Sci U S A. 1997; 94:8138–8143. [PubMed: 9223328]

Liu Y, Wada R, Kawai H, Sango K, Deng C, Tai T, McDonald MP, Araujo K, Crawley JN, Bierfreund U, Sandhoff K, Suzuki K, Proia RL. A genetic model of substrate deprivation therapy for a glycosphingolipid storage disorder. J Clin Invest. 1999; 103:497–505. [PubMed: 10021458]

Lukins TR, Tisch S, Jonker B. The latest evidence on target selection in deep brain stimulation for Parkinson's disease. Journal of clinical neuroscience : official journal of the Neurosurgical Society of Australasia. 2014; 21:22–27. [PubMed: 24210797]

Maiti P, Gregg LC, McDonald MP. MPTP-induced executive dysfunction is associated with altered prefrontal serotonergic function. Behav Brain Res. 2016; 298:192–201. [PubMed: 26393431]

Martinez Z, Zhu M, Han S, Fink AL. GM1 specifically interacts with α-synuclein and inhibits fibrillation. Biochemistry (Mosc). 2007; 46:1868–1877.

McCutcheon JE, Fisher AS, Guzdar E, Wood SA, Lightman SL, Hunt SP. Genetic background influences the behavioural and molecular consequences of neurokinin-1 receptor knockout. Eur J Neurosci. 2008; 27:683–690. [PubMed: 18279320]

McDonald MP, Miller KM, Li C, Deng C, Crawley JN. Motor deficits in fibroblast growth factor receptor-3 null mutant mice. Behav Pharmacol. 2001; 12:477–486. [PubMed: 11742142]

McKerchar TL, Zarcone TJ, Fowler SC. Use of a force-plate actometer for detecting and quantifying vertical leaping induced by amphetamine in BALB/cJ mice, but not in C57BL/6J, DBA/2J, 129X1/SvJ, C3H/HeJ, and CD-1 mice. J Neurosci Methods. 2006; 153:48–54. [PubMed: 16290200]

Melchiorri D, Martini F, Lococo E, Gradini R, Barletta E, De Maria R, Caricasole A, Nicoletti F, Lenti L. An early increase in the disialoganglioside GD3 contributes to the development of neuronal apoptosis in culture. Cell Death Differ. 2002; 9:609–615. [PubMed: 12032669]

Mitsumoto Y, Watanabe A, Mori A, Koga N. Spontaneous regeneration of nigrostriatal dopaminergic neurons in MPTP-treated C57BL/6 mice. Biochem Biophys Res Commun. 1998; 248:660–663. [PubMed: 9703982]

Mochizuki H, Goto K, Mori H, Mizuno Y. Histochemical detection of apoptosis in Parkinson's disease. J Neurol Sci. 1996; 137:120–123. [PubMed: 8782165]

Montkowski A, Poettig M, Mederer A, Holsboer F. Behavioural performance in three substrains of mouse strain 129. Brain Res. 1997; 762:12–18. [PubMed: 9262153]

Morales A, Colell A, Mari M, Garcia-Ruiz C, Fernandez-Checa JC. Glycosphingolipids and mitochondria: role in apoptosis and disease. Glycoconj J. 2004; 20:579–588. [PubMed: 15454696]

Newburn EN, Duchemin AM, Neff NH, Hadjiconstantinou M. GM1 ganglioside enhances Ret signaling in striatum. J Neurochem. 2014; 130:541–554. [PubMed: 24821093]

Norflus F, Tifft CJ, McDonald MP, Goldstein G, Crawley JN, Hoffmann A, Sandhoff K, Suzuki K, Proia RL. Bone marrow transplantation prolongs life span and ameliorates neurologic manifestations in Sandhoff disease mice. J Clin Invest. 1998; 101:1881–1888. [PubMed: 9576752]

Piochon C, Kloth AD, Grasselli G, Titley HK, Nakayama H, Hashimoto K, Wan V, Simmons DH, Eissa T, Nakatani J, Cherskov A, Miyazaki T, Watanabe M, Takumi T, Kano M, Wang SS, Hansel C. Corrigendum: Cerebellar plasticity and motor learning deficits in a copy-number variation mouse model of autism. Nat Commun. 2015; 6:6014. [PubMed: 25625889]

Porritt MJ, Batchelor PE, Howells DW. Inhibiting BDNF expression by antisense oligonucleotide infusion causes loss of nigral dopaminergic neurons. Exp Neurol. 2005; 192:226–234. [PubMed: 15698637]

Poulopoulos M, Cortes E, Vonsattel JP, Fahn S, Waters C, Cote LJ, Moskowitz C, Honig LS, Clark LN, Marder KS, Alcalay RN. Clinical and pathological characteristics of LRRK2 G2019S patients with PD. J Mol Neurosci. 2012; 47:139–143. [PubMed: 22194196]

Przedborski S, Jackson-Lewis V, Naini AB, Jakowec M, Petzinger G, Miller R, Akram M. The parkinsonian toxin 1-methyl-4-phenyl-1,2,3,6-tetrahydropyridine (MPTP): a technical review of its utility and safety. J Neurochem. 2001; 76:1265–1274. [PubMed: 11238711]

Ribeiro-Resende VT, Araujo Gomes T, de Lima S, Nascimento-Lima M, Bargas-Rega M, Santiago MF, Reis RA, de Mello FG. Mice lacking GD3 synthase display morphological abnormalities in the sciatic nerve and neuronal disturbances during peripheral nerve regeneration. PLoS One. 2014; 9:e108919. [PubMed: 25330147]

Rommelfanger KS, Edwards GL, Freeman KG, Liles LC, Miller GW, Weinshenker D. Norepinephrine loss produces more profound motor deficits than MPTP treatment in mice. Proc Natl Acad Sci U S A. 2007; 104:13804–13809. [PubMed: 17702867]

Rosenblad C, Georgievska B, Kirik D. Long-term striatal overexpression of GDNF selectively downregulates tyrosine hydroxylase in the intact nigrostriatal dopamine system. Eur J Neurosci. 2003; 17:260–270. [PubMed: 12542662]

Samantaray S, Knaryan VH, Shields DC, Cox AA, Haque A, Banik NL. Inhibition of Calpain Activation Protects MPTP-Induced Nigral and Spinal Cord Neurodegeneration, Reduces Inflammation, and Improves Gait Dynamics in Mice. Mol Neurobiol. 2015; 52:1054–1066. [PubMed: 26108182]

Sango K, McDonald MP, Crawley JN, Mack ML, Tifft CJ, Skop E, Starr CM, Hoffmann A, Sandhoff K, Suzuki K, Proia RL. Mice lacking both subunits of lysosomal β-hexosaminidase display gangliosidosis and mucopolysaccharidosis. Nat Genet. 1996; 14:348–352. [PubMed: 8896570]

Sango K, Yamanaka S, Hoffmann A, Okuda Y, Grinberg A, Westphal H, McDonald MP, Crawley JN, Sandhoff K, Suzuki K, Proia RL. Mouse models of Tay-Sachs and Sandhoff diseases differ in neurologic phenotype and ganglioside metabolism. Nat Genet. 1995; 11:170–176. [PubMed: 7550345]

Sauer H, Oertel WH. Progressive degeneration of nigrostriatal dopamine neurons following intrastriatal terminal lesions with 6-hydroxydopamine: a combined retrograde tracing and immunocytochemical study in the rat. Neuroscience. 1994; 59:401–415. [PubMed: 7516500]

Schneider JS. Chronic exposure to low doses of MPTP. II Neurochemical and pathological consequences in cognitively-impaired, motor asymptomatic monkeys. Brain Res. 1990; 534:25–36. [PubMed: 2073585]

Schneider JS. GM1 ganglioside in the treatment of Parkinson's disease. Ann N Y Acad Sci. 1998; 845:363–373. [PubMed: 9668369]

Schneider JS, Gollomp SM, Sendek S, Colcher A, Cambi F, Du W. A randomized, controlled, delayed start trial of GM1 ganglioside in treated Parkinson's disease patients. J Neurol Sci. 2013; 324:140–148. [PubMed: 23199590]

Schneider JS, Roeltgen DP. Delayed matching-to-sample, object retrieval, and discrimination reversal deficits in chronic low dose MPTP-treated monkeys. Brain Res. 1993; 615:351–354. [PubMed: 8364742]

Schneider JS, Roeltgen DP, Rothblat DS, Chapas-Crilly J, Seraydarian L, Rao J. GM1 ganglioside treatment of Parkinson's disease: an open pilot study of safety and efficacy. Neurology. 1995; 45:1149–1154. [PubMed: 7783880]

Schneider JS, Sendek S, Daskalakis C, Cambi F. GM1 ganglioside in Parkinson's disease: Results of a five year open study. J Neurol Sci. 2010; 292:45–51. [PubMed: 20206941]

Schneider JS, Seyfried TN, Choi HS, Kidd SK. Intraventricular Sialidase Administration Enhances GM1 Ganglioside Expression and Is Partially Neuroprotective in a Mouse Model of Parkinson's Disease. PLoS One. 2015; 10:e0143351. [PubMed: 26629687]

Schneider JS, Sun ZQ, Roeltgen DP. Effects of dihydrexidine, a full dopamine D-1 receptor agonist, on delayed response performance in chronic low dose MPTP-treated monkeys. Brain Res. 1994a; 663:140–144. [PubMed: 7850462]

Schneider JS, Sun ZQ, Roeltgen DP. Effects of dopamine agonists on delayed response performance in chronic low-dose MPTP-treated monkeys. Pharmacol Biochem Behav. 1994b; 48:235–240. [PubMed: 7913226]

Schneider JS, Yuwiler A. GM1 ganglioside treatment promotes recovery of striatal dopamine concentrations in the mouse model of MPTP-induced parkinsonism. Exp Neurol. 1989; 105:177–183. [PubMed: 2568945]

Siesser WB, Zhao J, Miller LR, Cheng SY, McDonald MP. Transgenic mice expressing a human mutant β1 thyroid receptor are hyperactive, impulsive, and inattentive. Genes, brain, and behavior. 2006; 5:282–297.

Smith BA, Goldberg NR, Meshul CK. Effects of treadmill exercise on behavioral recovery and neural changes in the substantia nigra and striatum of the 1-methyl-4-phenyl-1,2,3,6-tetrahydropyridine-lesioned mouse. Brain Res. 2011; 1386:70–80. [PubMed: 21315689]

Sora I, Hall FS, Andrews AM, Itokawa M, Li XF, Wei HB, Wichems C, Lesch KP, Murphy DL, Uhl GR. Molecular mechanisms of cocaine reward: combined dopamine and serotonin transporter knockouts eliminate cocaine place preference. Proc Natl Acad Sci U S A. 2001; 98:5300–5305. [PubMed: 11320258]

Stanford JA, Shuler JM, Fowler SC, Stanford KG, Ma D, Bittel DC, Le Pichon JB, Shapiro SM. Hyperactivity in the Gunn rat model of neonatal jaundice: age-related attenuation and emergence of gait deficits. Pediatr Res. 2015; 77:434–439. [PubMed: 25518009]

Stover KR, Campbell MA, Van Winssen CM, Brown RE. Analysis of motor function in 6-month-old male and female 3xTg-AD mice. Behav Brain Res. 2015; 281:16–23. [PubMed: 25486177]

Wang XH, Lu G, Hu X, Tsang KS, Kwong WH, Wu FX, Meng HW, Jiang S, Liu SW, Ng HK, Poon WS. Quantitative assessment of gait and neurochemical correlation in a classical murine model of Parkinson's disease. BMC neuroscience. 2012; 13:142. [PubMed: 23151254]

Wolfer DP, Muller U, Stagliar M, Lipp HP. Assessing the effects of the 129/Sv genetic background on swimming navigation learning in transgenic mutants: a study using mice with a modified beta-amyloid precursor protein gene. Brain Res. 1997; 771:1–13. [PubMed: 9383002]

Wu G, Lu ZH, Kulkarni N, Amin R, Ledeen RW. Mice lacking major brain gangliosides develop parkinsonism. Neurochem Res. 2011; 36:1706–1714. [PubMed: 21399908]

Wu G, Lu ZH, Kulkarni N, Ledeen RW. Deficiency of ganglioside GM1 correlates with Parkinson's disease in mice and humans. J Neurosci Res. 2012; 90:1997–2008. [PubMed: 22714832]

Wu G, Xie X, Lu ZH, Ledeen RW. Cerebellar neurons lacking complex gangliosides degenerate in the presence of depolarizing levels of potassium. Proc Natl Acad Sci U S A. 2001; 98:307–312. [PubMed: 11134519]

Yao D, McGonigal R, Barrie JA, Cappell J, Cunningham ME, Meehan GR, Fewou SN, Edgar JM, Rowan E, Ohmi Y, Furukawa K, Furukawa K, Brophy PJ, Willison HJ. Neuronal expression of GalNAc transferase is sufficient to prevent the age-related neurodegenerative phenotype of complex ganglioside-deficient mice. J Neurosci. 2014; 34:880–891. [PubMed: 24431446]

Zhao Q, Cai D, Bai Y. Selegiline rescues gait deficits and the loss of dopaminergic neurons in a subacute MPTP mouse model of Parkinson's disease. Int J Mol Med. 2013; 32:883–891. [PubMed: 23877198]

Zhao Q, Gao J, Li W, Cai D. Neurotrophic and neurorescue effects of Echinacoside in the subacute MPTP mouse model of Parkinson's disease. Brain Res. 2010; 1346:224–236. [PubMed: 20478277]

Zhou S, Davidson C, McGlynn R, Stephney G, Dobrenis K, Vanier MT, Walkley SU. Endosomal/ lysosomal processing of gangliosides affects neuronal cholesterol sequestration in Niemann-Pick disease type C. Am J Pathol. 2011; 179:890–902. [PubMed: 21708114]
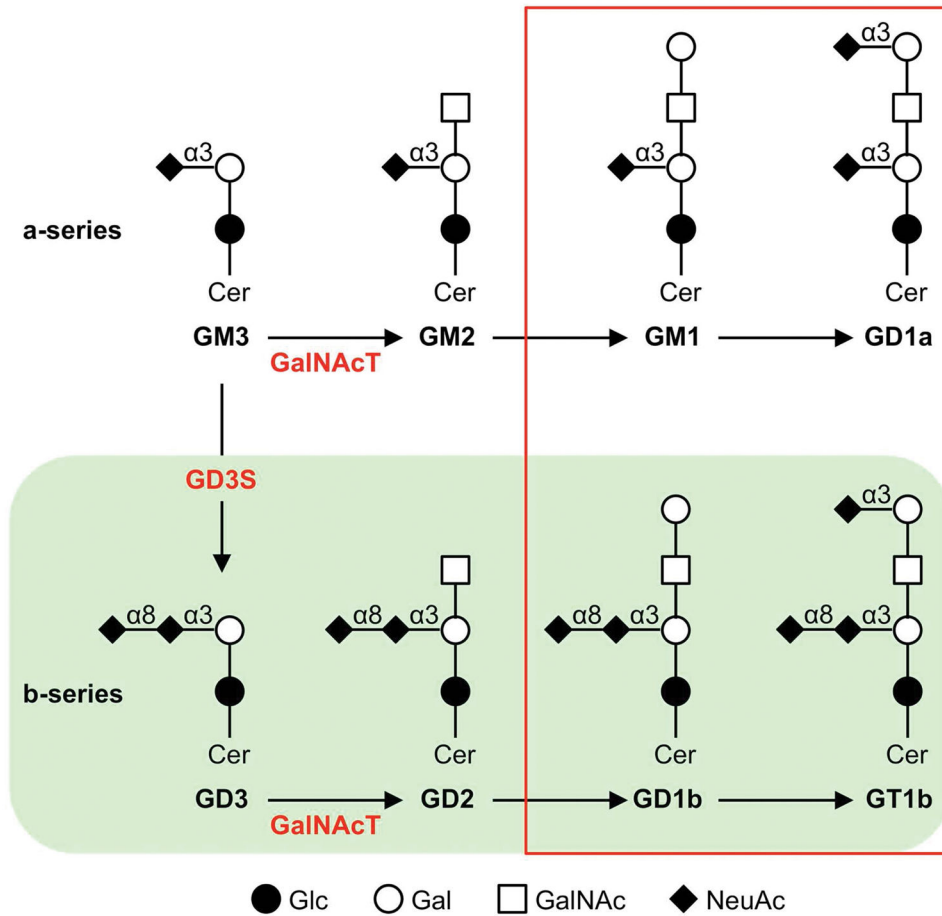
Figure 1. Ganglioside biosynthesis

Gangliosides are synthesized through sequential addition of carbohydrate moieties (mostly sialic acid and galactose) to a sphingosine backbone. The four major brain gangliosides (red box) comprise ~95% of total brain ganglioside. GD3S is responsible for synthesis of GD3 from GM3, so that knocking out GD3S eliminates the b-series gangliosides (green shading), including two of the four major brain gangliosides. However, we and others have shown that the total brain ganglioside in GD3S−/− mice is equivalent to that of wild-type controls, as constitutively high levels of GM3 ganglioside is converted to GM1 and GD1a rather than b-series gangliosides in the absence of GD3S (Bernardo *et al.*, 2009; Kawai *et al.*, 2001). Sialidase from *V. cholerae* (VCS) hydrolyzes α(2→8) and terminal α(2→3) sialic acid linkages, converting GD1a, GD1b, and GT1b to GM1 and producing a ganglioside profile similar to that of GD3S deletion but with greater levels of GM1 (Dhanushkodi & McDonald, 2011). GalNAcT is the enzyme coded by the *B4galnt1* gene and converts GM2 to GM1 and GD2 to GD1a. Abbreviations: Cer, ceramide; Glc, glucose; Gal, galactose; GalNAc, *N*-Acetylgalactosamine; NeuAc, N-Acetylneuraminic acid (sialic acid) GD3S, GD3 synthase; GalNAcT, GalNAc transferase; α3, α(2→3); α8, α(2→8).
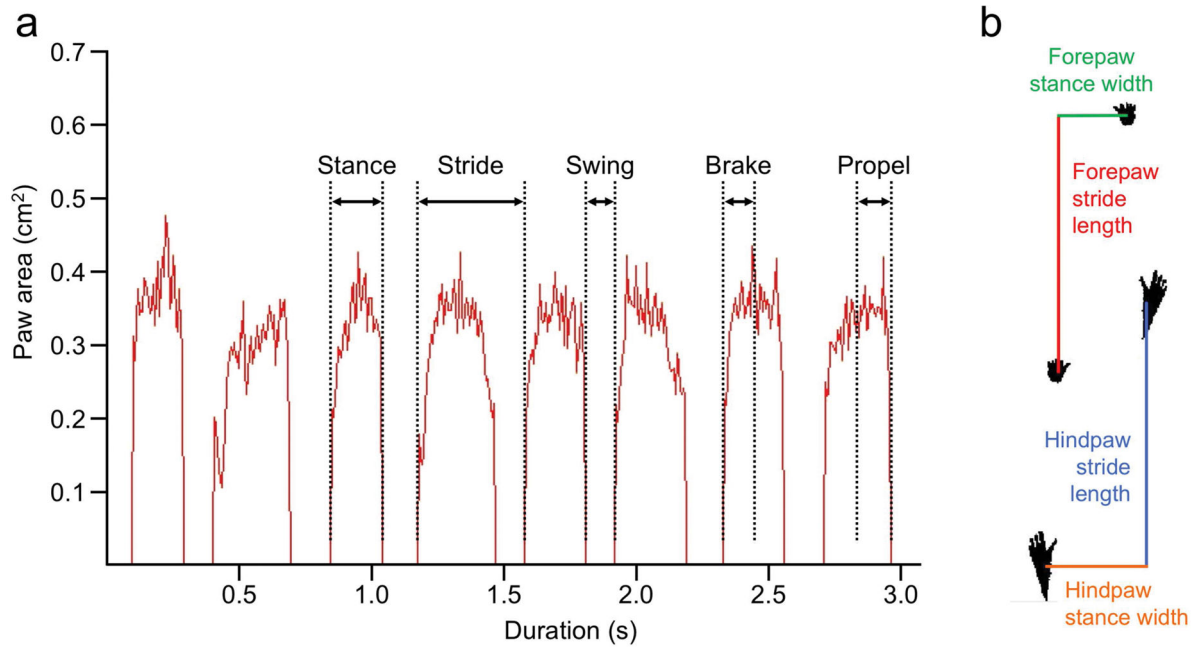
Figure 2. Gait measures on the DigiGait apparatus

a) Representative dynamic gait signals for duration of forepaw stride and the four stride components with a belt speed of 20 cm/s: brake, stance, propel, and swing. **b**) Paw print diagram depicting stance widths and stride lengths.
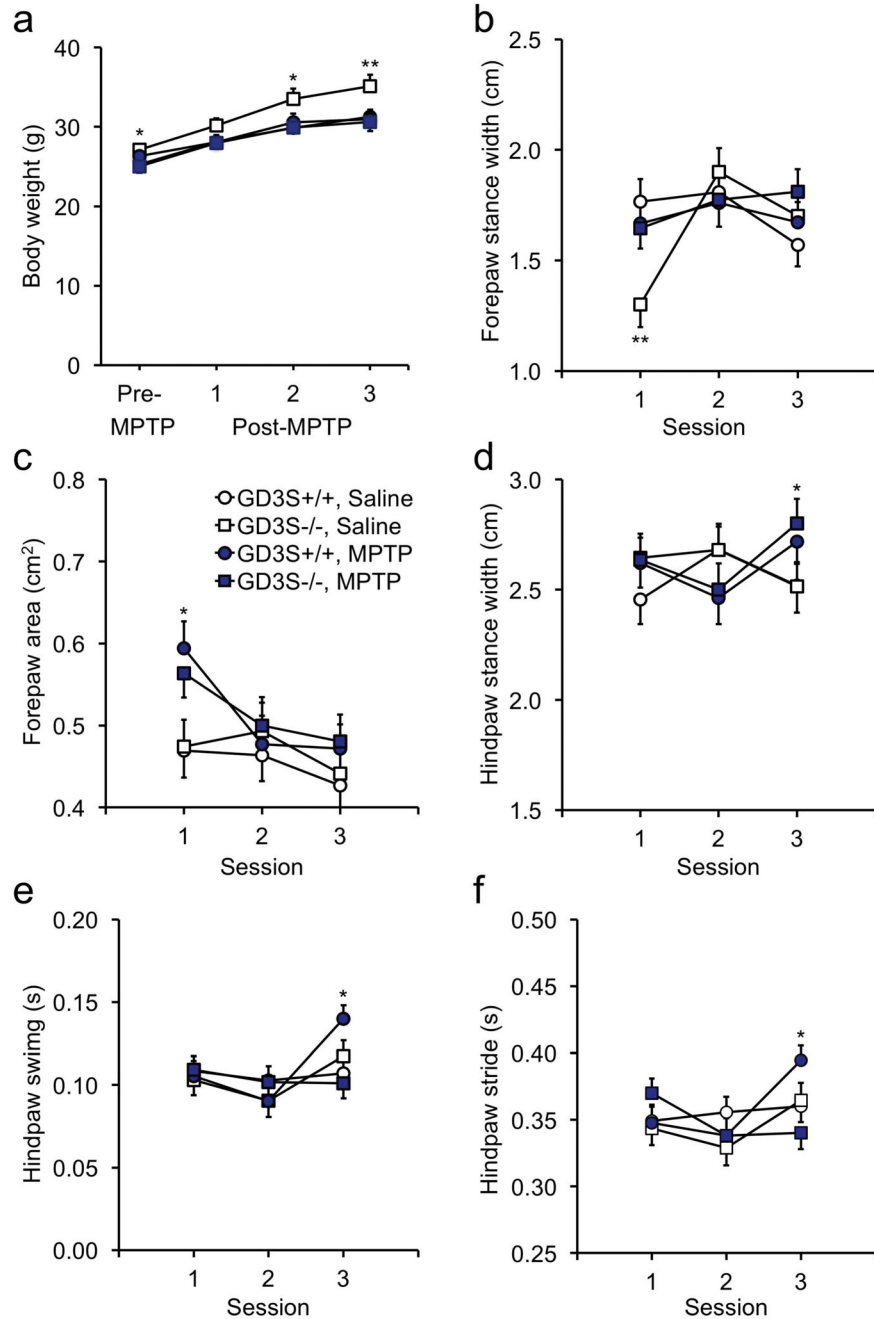
Figure 3. Repeated low-dose MPTP induces mild gait deficits

a) GD3S−/− mice assigned to the saline group were heavier from the beginning of the study, a difference that increased as the study progressed. The weights of the other three groups were virtually identical. Because body weight can affect performance on many motor tasks, it was used as a covariate when appropriate (see Statistics section). **b**) The forepaw stance width was significantly lower in GD3S−/− mice treated with saline, but only on the first session. **c**) MPTP-lesioned mice of both genotypes had greater forepaw angles only on the first session. **d**) After the third MPTP regimen, lesioned mice walked with a greater hindpaw

stance width. There was no genotype difference on this measure. In contrast, the hindpaw swing (**e**) and stride (**f**) were slower in MPTP-lesioned wild-type mice after three MPTP injection regimens, but GD3S−/− mice were unaffected by MPTP. Data are expressed as mean ± SEM. *p < .05; **p < .01; ***p < .001; ****p < .0001.
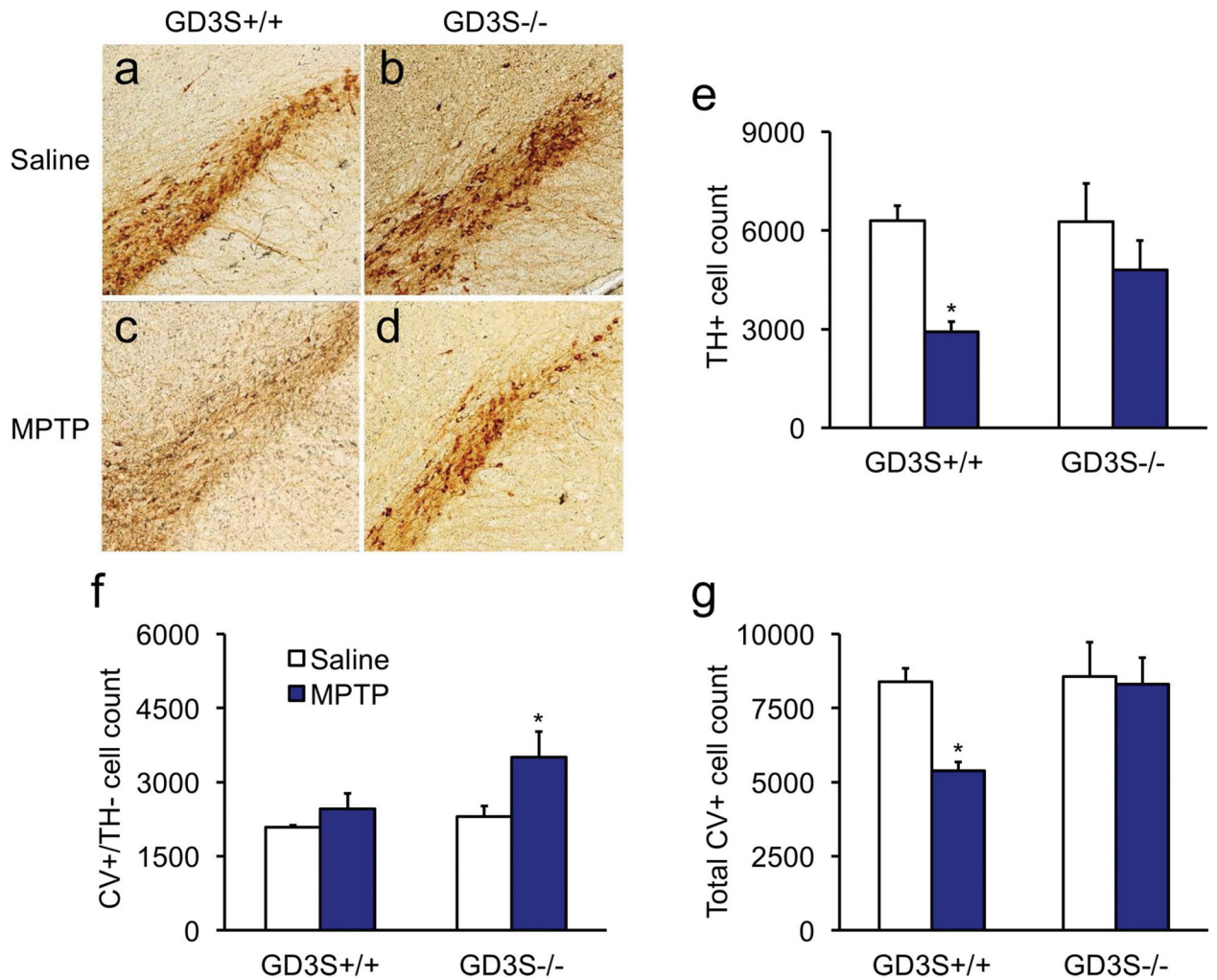
Figure 4. Tyrosine hydroxylase expression is partially suppressed in GD3S–/– mice

a,c,e) Wild-type mice lost 53.0 ± 4.8% of the TH+ neurons in the SNc after the third MPTP injection regimen. **b,d,e**) GD3S knockouts had a 22.5 ± 14.6% reduction of TH+ neurons, which was not statistically significant. **f**) Interestingly, GD3S–/– mice lesioned with MPTP had more CV-positive neurons in the SNc that were negative for TH. **g**) The total CV+ neurons (positive or negative for TH) did not differ in GD3S–/– mice compared to their saline-treated controls, suggesting that TH expression was suppressed in surviving SNc neurons. Data are expressed as mean ± SEM. *p < .05.
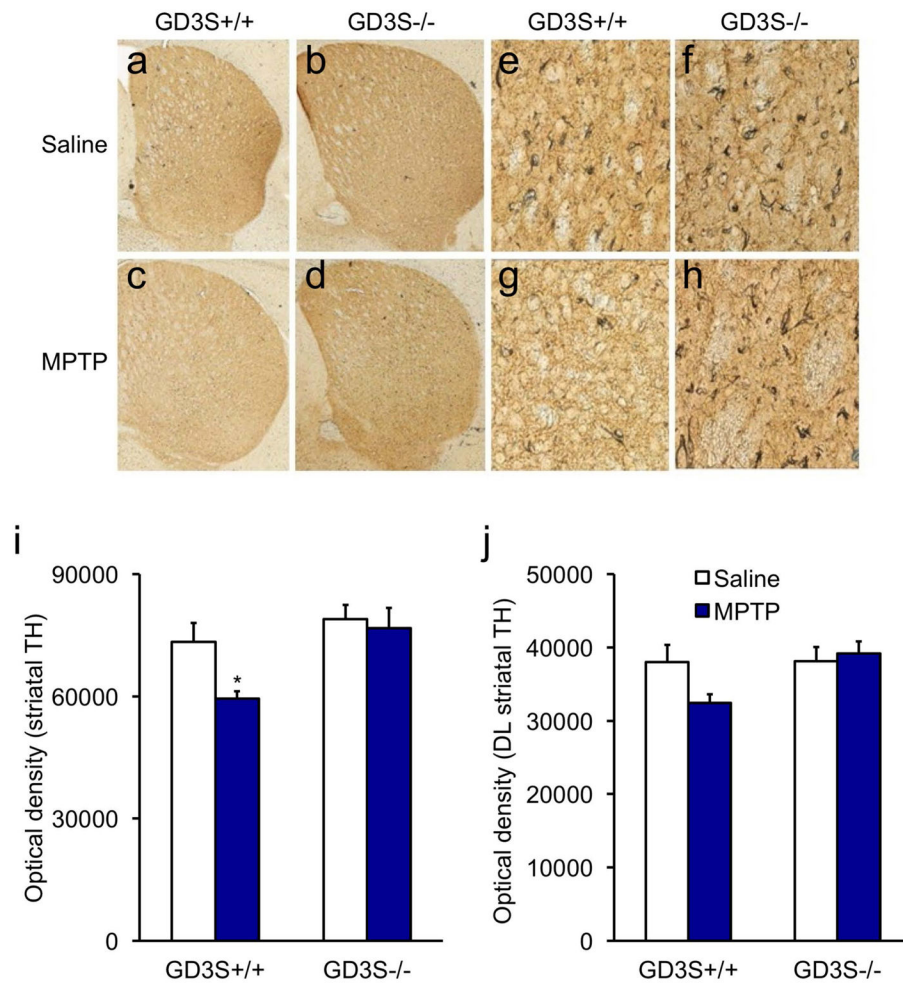
Figure 5. Striatal TH fiber density is restored in GD3S–/– mice
a,b) Immunohistochemistry revealed significantly-reduced TH+ fibers in the whole striatum
(**a-d**) and dorsolateral (DL) quadrant (**e-h**) of MPTP-lesioned wild-type but not GD3S–/–
mice. Densitometric analysis showed that MPTP reduced TH+ fibers by ~18% and ~15% in
the (**g**) whole striatum and (**h**) dorsolateral quadrant, respectively. Striatal TH+ fiber density
was not significantly affected by MPTP in GD3S–/– mice. Data are expressed as mean ±
SEM. *p < .05.

Table 1

Data (mean ± SEM) from sensorimotor tests collapsed across sessions.

Measure	GD3S+/+		GD3S−/−	
	Saline	**MPTP**	**Saline**	**MPTP**
Vertical screen (s)	2.95 ± 0.27	3.25 ± 0.48	3.75±0.48	2.96 ± 0.28
Step down (s)	8.55 ± 1.12	7.08 ± 0.80	12.92 ± 3.56	10.58 ± 1.77
Rotorod (s)	62.48 ± 7.03	65.40 ± 8.35	50.43 ± 7.22	55.46 ± 6.62
Grip strength				
Four paws (N)	0.33 ± 0.02	0.32 ± 0.02	0.34 ± 0.01	0.36 ± 0.01
Forepaws (N)	0.33 ± 0.02	0.31 ± 0.02	0.31 ± 0.01	0.28 ± 0.01
Activity monitors				
Distance traveled (m)	14.20 ± 2.73	14.62 ± 1.41	12.55 ± 1.71	12.24 ± 1.69
Rearing (count)	33.00 ±10.77	25.38 ± 6.93	17.90 ± 4.58	18.72 ± 5.04
Velocity (cm/s)	13.59 ± 1.09	12.68 ± 0.94	12.53 ± 1.02	12.86 ± 1.53
[1] Horizontal beam				
Latency to start (s)	3.25 ± 0.73	1.52 ± 0.14 [*]	2.32 ± 0.38	1.55 ± 0.17
Latency to traverse (s)	4.32 ± 0.30	4.18 ± 0.25	5.12 ± 0.25	3.62 ± 0.21 [^]
Sticker removal				
Latency to first attempt (s)	2.86 ± 0.67	3.29 ± 0.86	1.49 ± 0.18 [^]	1.31 ± 0.08 [^]
Latency to remove (s)	1.61 ± 0.20	2.07 ± 0.32	1.44 ± 0.19	1.54 ± 0.30

[1] Body weight was not included as a covariate in this model because of regression slope heterogeneity.

[*] $p < .05$ vs. respective saline control.

[^] $p < .05$ vs. respective wild-type control.

Table 2

Mean ± SEM locomotor activity from the force plate actimeter.

Measure	GD3S+/+		GD3S−/−	
	Saline	**MPTP**	**Saline**	**MPTP**
Long runs	8.27 ± 0.84	5.08 ± 0.94 [*]	4.91 ± 0.87 [^]	5.08 ± 0.98
Crossings	20.91 ± 3.04	12.67 ± 1.56 [*]	12.64 ± 1.97 [^]	14.92 ± 3.44
Total distance (m)	9.79 ± 1.06	8.14 ± 0.77	6.67 ± 0.67 [^]	8.62 ± 1.38
Bouts of low mobility	14.27 ± 1.76	13.67 ± 2.18	26.36 ± 2.92 [^^]	20.92 ± 3.15
Stride rate (Hz)	3.46 ± 0.09	3.39 ± 0.15	3.08 ± 0.16	3.31 ± 0.12
Stride length (mm)	62.58 ± 2.18	63.89 ± 2.45	64.70 ± 1.75	62.15 ± 1.34
Velocity (mm/s)	216.57 ±10.55	218.07 ±14.27	199.09 ±11.14	206.38 ±10.32
Integrated power (arbitrary units/1000)	5.10 ± 0.85	5.23 ± 0.70	3.91 ± 0.43 [^]	3.30 ± 0.28 [^]

Note: Integrated power was derived from periods of time when the subject was not locomoting, i.e., bouts of low mobility.

[*]
$p < .05$ vs. respective saline control.

[^]
$p < .05$;

[^^]
$p < .01$ vs. respective wild-type control.

Table 3

Data (mean ± SEM) from the gait analysis, collapsed across sessions.

Measure	GD3S+/+		GD3S−/−	
	Saline	MPTP	Saline	MPTP
Forepaws:				
Stance width (cm)	1.70 ± 0.06	1.68 ± 0.09	1.64 ± 0.05	1.72 ± 0.04
Step angle (°)	67.87 ± 2.13	66.29 ± 2.24	63.37 ± 1.61	63.54 ± 1.85
Stance (s)	0.22 ± 0.01	0.23 ± 0.01	0.23 ± 0.00	0.23 ± 0.01
Stride (s)	0.36 ± 0.01	0.35 ± 0.01	0.34 ± 0.01	0.34 ± 0.01
Swing (s)	0.13 ± 0.01	0.12 ± 0.01	0.11 ± 0.01 [^]	0.11 ± 0.00
Brake (s)	0.14 ± 0.00	0.14 ± 0.00	0.13 ± 0.01	0.13 ± 0.00
Propel (s)	0.09 ± 0.00	0.09 ± 0.00	0.09 ± 0.01	0.09 ± 0.01
Paw angle (°)	6.87 ± 0.66	4.52 ± 0.47 [**]	5.67 ± 0.81	4.61 ± 0.56
Paw Area (cm^2)	0.45 ± 0.01	0.51 ± 0.02 [*]	0.46 ± 0.02	0.53 ± 0.02
Hindpaws:				
Stance width (cm)	2.56 ± 0.07	2.64 ± 0.08	2.58 ± 0.05	2.64 ± 0.05
Step angle (°)	55.78 ± 1.77	57.23 ± 1.51	58.10 ± 1.25	58.09 ± 1.33
Stance (s)	0.25 ± 0.00	0.25 ± 0.00	0.24 ± 0.00	0.25 ± 0.00
Stride (s)	0.36 ± 0.01	0.37 ± 0.01	0.34 ± 0.01	0.35 ± 0.01
Swing (s)	0.11 ± 0.00	0.12 ± 0.01	0.10 ± 0.00	0.11 ± 0.00
Brake (s)	0.06 ± 0.00	0.06 ± 0.00	0.06 ± 0.00	0.05 ± 0.00
Propel (s)	0.19 ± 0.00	0.19 ± 0.00	0.18 ± 0.00	0.19 ± 0.00
Paw angle (°)	10.28 ± 0.62	10.52 ± 0.83	11.73 ± 1.34	11.32 ± 0.76
Paw area (cm^2)	0.81 ± 0.03	0.92 ± 0.05	0.84 ± 0.05	0.86 ± 0.05

[*] $p < .05$;

[**] $p < .01$ vs. respective saline control.

[^] $p < .05$;

[^^] $p < .01$ vs. respective wild-type control.

Table 4

Monoamine and metabolite levels (mean ± SEM) in the striatum

Abbreviations: DOPAC, 3, 4-dihydroxyphenylacetic acid; HVA, homovanillic acid; 3-MT, 3-methoxytyramine; DA, dopamine; DHPG, 3,4-dihydroxyphenylglycol; NE, norepinephrine; 5-HT, serotonin; 5-HIAA, 5-hydroxyindoleacetic acid.

Measure	GD3S+/+		GD3S−/−	
	Saline	MPTP	Saline	MPTP
Dopamine	9.16 ± 1.01	3.60 ± 0.46 [****]	9.37 ± 0.92	5.76 ± 0.73 [**]
DOPAC	0.44 ± 0.05	0.23 ± 0.03 [*]	0.52 ± 0.09	0.30 ± 0.04 [**]
HVA	0.72 ± 0.10	0.56 ± 0.06	0.83 ± 0.09	0.70 ± 0.09
3-MT	0.33 ± 0.04	0.21 ± 0.02 [*]	0.27 ± 0.03	0.30 ± 0.05
DOPAC/DA	0.05 ± 0.01	0.07 ± 0.01	0.05 ± 0.01	0.05 ± 0.00
HVA/DA	0.09 ± 0.02	0.16 ± 0.01 [****]	0.09 ± 0.01	0.012 ± 0.01 [*]
3-MT/DA	0.04 ± 0.01	0.06 ± 0.00 [***]	0.03 ± 0.00	0.05 ± 0.01 [***^]
Norepinephrine	1.12 ± 0.18	0.94 ± 0.17	1.15 ± 0.29	1.59 ± 0.39
DHPG	1.70 ± 0.18	1.41 ± 0.15	2.22 ± 0.38	1.41 ± 0.11
DHPG/NE	2.73 ± 0.69	2.51 ± 0.84	3.50 ± 1.07	3.10 ± 0.97
DA/NE	10.68 ± 2.47	4.73 ± 0.787 [**]	11.24 ± 1.556	6.00 ± 1.279 [*]
5-HT	0.25 ± 0.03	0.24 ± 0.03	0.34 ± 0.081	0.37 ± 0.055
5-HIAA	0.24 ± 0.029	0.24 ± 0.031	0.27 ± 0.055	0.29 ± 0.042
5-HIAA/5-HT	1.01 ± 0.061	1.04 ± 0.104	0.83 ± 0.091	0.80 ± 0.054 [^]

[*]
$p < .05$;

[**]
$p < .01$;

[***]
$p < .001$;

[****]
$p < .0001$ vs. respective saline control.

[^]
$p < .05$ vs. respective wild-type control.